For publication in Journal of Virology

Mutations in a highly conserved motif of nsp1β protein attenuate the innate immune suppression function of porcine reproductive and respiratory syndrome virus (PRRSV)

Yanhua Li[1a], *Duan-Liang Shyu*[2a], *Pengcheng Shang*[1], *Jianfa Bai*[1], *Kang Ouyang*[2], *Santosh Dhakal*[2], *Jagadish Hireamt*[2], *Basavaraj Binjawadagi*[2], *Gourapura J. Renukaradhya*[2]*, *Ying Fang*[1]*

1. Department of Diagnostic Medicine and Pathobiology, College of Veterinary Medicine, Kansas State University, Manhattan, KS 66506.

2. Food Animal Health Research Program (FAHRP), Veterinary Preventive Medicine, The Ohio State University, Wooster, OH 44691.

*To whom correspondence should be addressed. E-mail: gourapura.1@osu.edu; yfang@vet.k-state.edu.

[a]Yanhua Li and Duan-Liang Shyu contribute equally to this work.

Running title: PRRSV nsp1β mutation and attenuation *in vivo*

Abstract word count: 250

Main text word count: 9933

ABSTRACT

PRRSV nonstructural protein 1β (nsp1β) is a multifunctional viral protein, which involves in suppressing innate immune response and activating a unique -2/-1 programmed ribosomal frameshifting (PRF) signal for the expression of frameshifting products. In this study, site-directed mutagenesis analysis showed that R128A or R129A mutation introduced in a highly conserved motif ($_{123}$GKYLQRRLQ$_{131}$) reduced the ability of nsp1β to suppress IFN-β activation and also impaired nsp1β's function as PRF transactivator. Three recombinant viruses, vR128A, vR129A and vRR129AA, carrying single or double mutations in the GKYLQRRLQ motif were characterized. In comparison to the wild type (WT) virus, vR128A and vR129A showed slightly reduced growth ability, while vRR129AA mutant had significantly reduced growth ability in infected cells. Consistent with the attenuated growth phenotype *in vitro*, the pigs infected with nsp1β mutants had lower level of viremia than that of WT virus-infected pigs. Comparing to WT virus in infected cells, all of the three mutated viruses stimulated higher level of IFN-α expression and exhibited reduced ability in suppressing mRNA expression of selected ISGs. In pigs infected with nsp1β mutants, IFN-α production was increased in the lungs during early time points of post-infection, which was correlated with an increased innate NK cell function. Furthermore, augmented innate response was consistent with increased production of IFN-γ in those mutated viruses-infected pigs. These data demonstrate that R128 and R129 residues are critical for nsp1β function, and modifying these key residues in the GKYLQRRLQ motif attenuates virus growth ability and improve the innate and adaptive immune responses in infected animals.

IMPORTANCE

PRRSV infection induces poor anti-viral innate IFN and cytokine responses, which results in weak adaptive immunity. One of the strategies in next generation vaccine construction is to manipulate viral proteins/genetic elements involved in antagonizing host immune response. The PRRSV nsp1β was identified to be a strong innate immune antagonist. In this study, two basic amino acids, R128 and R129, in a highly conserved GKYLQRRLQ motif were determined to be critical for nsp1β function. Mutations introduced into these two residues attenuated virus growth and improved the innate and adaptive immune responses in infected animals. Technologies developed in this study could be broadly applied to current commercial PRRSV MLV vaccines and other candidate vaccines.

INTRODUCTION

Porcine reproductive and respiratory syndrome (PRRS), a disease described in the US in 1987 (1) and in Europe in 1990 (2), has caused tremendous economic losses to the swine industry since its appearance. Hallmark symptoms of PRRS are mild to severe respiratory disease in infected newborn and growing pigs, and reproductive failure in pregnant sows. The etiologic agent, PRRS virus (PRRSV), was first discovered in the Netherlands in 1991 (2). In the US, PRRSV was first isolated and characterized in 1992 (3, 4). Generally, infection of pigs by most of the PRRSV strains dampens the host innate immune response (5, 6). This initial suppression of host innate immune response, leading to the delayed induction of protective cellular and humoral immunity (7, 8), which provides a window of time that allows PRRSV to replicate, shed and transmit to other contact naïve animals. Therefore, strategies for vaccine development are directed at constructing a PRRS vaccine capable of inducing a high level of innate and adaptive immune responses.

PRRSV is an enveloped, positive-stranded RNA virus, which belongs to the order *Nidovirales,* family *Arteriviridae,* including equine arteritis virus (EAV), mouse lactate dehydrogenase-elevating virus (LDV), simian hemorrhagic fever virus (SHFV) and several recently discovered monkey arteriviruses that are only distantly related to SHFV (9). The PRRSV genome is about 15kb in length and contains at least eleven open reading frames. The 3' end of the genome encodes four membrane-associated glycoproteins (GP2a, GP3, GP4 and GP5), three unglycosylated membrane proteins (E, ORF5a and M) and a nucleocapsid protein (N) (10-19). The replicase-associated genes, ORF1a and ORF1b, situated at the 5' end, and represent nearly 75% of the viral genome. The ORF1a and ORF1b encode two large polyproteins, pp1a and pp1ab, with expression of the latter depending on a -1 ribosomal frameshifting signal in the

85 ORF1a/ORF1b overlap region. Following their synthesis from the genomic mRNA template, the
86 pp1a and pp1ab replicase polyproteins are processed into at least 14 nonstructural proteins (nsps)
87 by a complex proteolytic cascade that is directed by four proteinase domains encoded in ORF1a,
88 which include two papain-like proteinases (PLP1α and PLP1β) located in the nsp1α and nsp1β, a
89 papain-like proteinase (PLP2) domain located at the N-terminal of nsp2, and a serine proteinase
90 located in nsp4. The PLPα auto-cleaves between nsp1α/1β, PLPβ auto-cleaves between nsp1β/2,
91 and PLP2 cleaves between nsp2/3, which mediate the rapid release of nsp1α, nsp1β and nsp2
92 from the polyprotein (20). Recently, two novel PRRSV proteins, nsp2TF and nsp2N, were
93 identified (21). The nsp2TF and nsp2N are expressed by a novel -2/-1 programmed ribosomal
94 frameshifting (PRF) mechanism, which accesses the alternative ORF (TF) through a
95 frameshifting site that overlaps the nsp2-encoding region. Both nsp2TF and nsp2N share the N-
96 terminal 2/3 sequence with nsp2, which contains the PLP2 domain.

97 Previous studies from our laboratory and others identified PRRSV nsp1β to be a strong innate
98 immune antagonist (22-24). PRRSV nsp1β has strong inhibitory effects on type I IFN production
99 and signaling pathways that lead to the expression of interferon stimulated genes (ISGs).
100 Interestingly, this protein was recently identified to also function as a transactivator for the
101 expression of -2/-1 PRF products, nsp2TF and nsp2N (25). Embedded in nsp1β's papain-like
102 autoproteinase domain (PLP1β), a highly conserved GKYLQRRLQ motif was identified to be
103 critical for -2/-1 PRF transactivation and innate immune suppression function of the virus (25,
104 26). Based on the crystal structure analysis, three basic residues (K124, R128, and R129) in
105 GKYLQRRLQ motif are exposed on the surface of the protein (25). In this study, we further
106 investigated the function of the basic residues K124, R128, and R129 involved in modulation of

host immune responses. Recombinant viruses carrying mutations in these basic residues were created and characterized in cell culture systems as well as in a nursery piglet model.

MATERIALS AND METHODS

Cells and viruses. HEK-293T cells and MARC-145 cells were maintained in minimum essential medium (Gibco) supplemented with 10% fetal bovine serum and antibiotic (Streptomycin, 100 μg/mL) at 37 ^{o}C with 5% CO_2. BHK-21 cells were cultured in minimum essential medium supplemented with 5% fetal bovine serum and antibiotic (Streptomycin, 100 μg/mL). As described previously, porcine alveolar macrophages were obtained from lung lavage of 6-week-old PRRSV naive piglets (27). The Sendai virus (SeV), Cantell strain, grown in embryonated chicken eggs was used for stimulation of type 1 IFN response in cell culture system. The type 2 PRRSV isolate SD95-21 (GenBank accession: KC469618), and its nsp1β mutants were used for subsequent experiments.

Antibodies. To detect the expression of nsp1β and its mutants, mAb 123-128 (25) or the anti-FLAG M2 mAb (Sigma-Aldrich, St. Louis, MO) was used. The mAb 140-68 (25), specifically recognizing the common N-terminal PLP2 domain of nsp2, nsp2TF and nsp2N, was used to detect the expression of nsp2-related proteins. The rabbit pAb against nsp2TF (25) was utilized to immunoprecipitate and detect nsp2TF. In addition, the anti-β-tubulin mAb (abm Inc., BC, Canada) was used to detect the expression of housekeeping gene β-tubulin. Antibody mixture of mAb M2 against FLAG and anti-β-tubulin was used for simultaneously detection the expression of FLAG-tagged nsp1β and β-tubulin in western blot, while antibody mixture of mAb 123-128 and anti-β-tubulin was used for simultaneously detection the expression of nsp1β and β-tubulin in western blot.

130 *Plasmids.* Using the nsp1β expressing plasmid (p3xFLAG-NA-nsp1β) that we generated
131 previously (26), specific mutations, K124A, R128A, R129A, or RR129AA (double mutations of
132 R128A and R129A) in the GKYLQRRLQ motif region (amino acids 123-131) of nsp1β were
133 introduced by site-directed mutagenesis using QuickChange™ site-directed mutagenesis kit
134 (Agilent Technologies, Inc., Santa Clara, CA), following the manufacturer's instruction. A
135 vaccinia/T7 polymerase system (pL-NA-nsp1β-2) expressing the nsp1β-nsp2 of SD95-21 virus
136 was described previously (26). Specific mutations (K124A, R128A, R129A, or RR129AA) were
137 introduced into the nsp1β region of pL-NA-nsp1β-2 using QuickChange™ site-directed
138 mutagenesis kit. To generate full-length PRRSV cDNA clones containing these specific
139 mutations (R128A, R129A, or RR129AA), a shuttle plasmid carrying the region between two
140 unique restriction sites (Sph *I* and Sca *I*) of the full-length cDNA clone of PRRSV (pCMV-
141 SD95-21) was constructed using Zero Blunt® PCR Cloning Kit (Invitrogen, Carlsbad, CA).
142 QuickChange™ site-directed mutagenesis kit (Agilent Technologies, Inc., Santa Clara, CA) was
143 employed to introduce the specific mutations into the shuttle plasmid. The region between Sph*I*
144 and Sca*I* of pCMV-SD95-21 was replaced by the corresponding regions of the shuttle plasmids
145 containing the specific mutations. The mutated full-length cDNA clones were designated as
146 pCMV-SD95-21-R128A, pCMV-SD95-21-R129A, and pCMV-SD95-21-RR129AA. DNA
147 sequencing was further performed to verify the introduced mutations. For *in vitro* luciferase
148 reporter assay, two reporter plasmids, the p125-Luc and pISRE-Luc, were used as described
149 previously (26).

150 *Luciferase reporter assay.* HEK-293T cells were seeded at 0.5×10^5 cells/mL in 24-well plates
151 one day before transfection. DNA transfection was conducted using FuGENE HD transfection
152 reagent (Promega, Madison, WI). Briefly, cells were co-transfected with 0.5 μg plasmid DNA

153 expressing WT nsp1β (or its mutants) and 0.5 μg luciferase reporter plasmid DNA of p125-Luc
154 or pISRE-Luc. At 24 h post-transfection, cells were mock treated or stimulated with the SeV
155 inoculated at 100 HA unit/ml/well for 16 h, or treatment with IFN-β at 2000 IU/ml/well for 16 h.
156 Cells were lysed and used for reporter gene assay using the dual luciferase reporter system
157 (Promega, Madison, WI) according to the manufacturer's instruction. Firefly luciferase activities
158 were measured with FLUOstar Omega (BMG LABTECH, Cary, NC).

159 *Vaccinia/T7 polymerase expression system.* The nsp1β-nsp2 and its mutants were expressed
160 using a vaccinia/T7 polymerase system (28) as described previously (26). Briefly, HEK-293T
161 cells ($1x10^6$/well) were seeded in 6-well plates one day before infection. Cells in each of the well
162 were infected with a vaccinia virus expressing T7 polymerase at a multiplicity of infection (MOI)
163 of 10. At 1 h post-infection, cells were transfected with 2μg DNA of pL-NA-nsp1β-2 or its
164 mutants using FuGENE HD transfection reagent (Promega, Madison, WI). At 18 h post-
165 transfection, cell lysate from each well of 6-well plate was harvested and subjected to western
166 blot analysis using antibodies against nsp1β (mAb 123-128) and nsp2 (mAb 140-68). In addition,
167 cell lysate was used in immunoprecipitation to evaluate the expression of -2 PRF product with
168 the antibody that specifically recognizes nsp2TF (pAb-TF).

169 *Western Blot Analysis.* Western blot analysis was performed to evaluate protein expression using
170 the method described previously (20, 26). Briefly, cell lysates were prepared by harvesting virus-
171 infected or plasmid DNA-transfected cells with RIPA buffer. Cell lysate was mixed with equal
172 volume of Laemmli sample buffer and heated at 95 ^{o}C for 6 min. After being separated by
173 sodium dodecyl sulfate-polyacrylamide gel electrophoresis (SDS-PAGE), proteins were
174 transferred onto a nitrocellulose membrane. The membrane was blocked with 5% skim milk in
175 PBST (PBS with 0.05% Tween 20) at 4 ^{o}C overnight, and then incubated with primary antibody

at appropriate dilution at room temperature for 1h. After 3 times wash with PBST, the secondary antibody, IRDye® 800CW Goat anti-Mouse IgG (H + L) or/and IRDye® 680RD Goat anti-Rabbit IgG (H + L) (LI-COR Biosciences, Lincoln, NE), was added and the membrane was incubated for additional 1 h at room temperature. The target proteins were visualized and quantified using a digital image system (Odyssey infrared imaging system; LI-COR Biosciences, Lincoln, NE). For quantification of the target proteins, the expression levels were normalized to the expression level of β-tubulin, which is a house keeping gene used as a loading control.

Recovery of recombinant viruses from infectious cDNA clones. The procedure for generating recombinant viruses was described previously (26). BHK-21 cells with 70-80% confluency were transfected with 2 μg of the type 2 PRRSV full-length cDNA clone of pCMV-SD95-21 or the full-length cDNA clones containing nsp1β mutations. Transfection was performed using FuGENE HD reagent (Promega, Madison, WI). At 48 h post-transfection, cell culture supernatant was harvested and passaged onto MARC-145 cells. After 48-60 h of incubation, indirect immunofluorescence assay were performed to confirm the viability of recombinant viruses using mAb SDOW17 (PRRSV N protein-specific monoclonal antibody, (29)). The recombinant viruses were serially passaged on MARC-145 cells, and passage 3 and 4 viruses were used for further analysis.

Sequencing of nsp1β mutation regions. To determine the stability of each mutation, cell culture supernatant from recombinant virus-infected cells or serum samples collected from experimentally infected animals [14, 21 and 35 days post infection (DPI)] were used for viral RNA extraction using the QIAamp viral RNA kit (QIAGEN). The nsp1β coding region containing the corresponding mutations was amplified by RT-PCR, and PCR products were subjected to DNA sequencing at GENEWIZ, Inc. (South Plainfield, NJ).

Virus growth kinetics and plaque assay. The passage 3 of WT and mutant viruses were used to characterize viral growth properties *in vitro*. Confluent MARC-145 cells were inoculated with WT virus or nsp1β mutants at a MOI of 0.01. Cell culture supernatant was harvested at 12, 24, 36, 48, 60, 72 h post-infection. Virus titer was measured by micro-titration assay using MARC-145 cells in 96-well plates and calculated as $TCID_{50}$/ml according to the Reed and Muench method (30). To determine the plaque morphology of WT virus and nsp1β mutants, plaque assay was conducted using MARC-145 cells as described previously (31).

Pig groups, sample collection and preparation. A total of 45 specific pathogen free (SPF) pigs were obtained from the swine farm of The Ohio State University. Pigs were randomly divided into 5 groups (n=9; Table 1). Pigs were mock-infected (group 1), or infected with $4x10^6$ $TCID_{50}$ of WT PRRSV (group 2), vR128A mutant (group 3), vR129A mutant (group 4), vRR129AA mutant (group 5). The virus was inoculated through both intranasal (IN) and intramuscular (IM) routes with 1mL ($1x10^6$ $TCID_{50}$) of the virus suspension in MEM to each nostril and to each side of the neck. Pigs were observed daily and blood samples were collected on 0, 1, 2, 5, 7, 14, 21, 28, 35 DPI. Three pigs from each group were sequentially euthanized at 7, 21, and 35 DPI (Table 1). During necropsy, the lungs were evaluated for gross lesions using the method described previously (32), and bronchoalveolar lavage fluid (BALF) and lung tissue samples were collected as described previously (33). The pig experiment was performed according to the protocol approved by the Institutional Animal Care and Use Committee (IACUC) of The Ohio State University, Ohio.

Real-time RT-PCR quantification of viral load in infected animals. For the determination of viral RNA load, serum, BALF and lung lysate samples were examined using a real-time quantitative RT-PCR. Briefly, viral genomic RNA was extracted using MagMAX™-96 viral RNA isolation

kit (life technologies) following the manufacturer's instruction. Viral RNA level was determined by a quantitative RT-PCR using iTaq™ Universal SYBR® Green One-Step Kit (Bio-Rad, Hercules, CA), and the RNA copy numbers were calculated based on a RNA standard curve. A pair of primers, PRRS-qF1 (CCATTTCCTTGACACAGTCG) and PRRS21-qR2 (GACCGCGTAGATGCTACTTAGG) located at viral genomic region (nt 14043-14130), was designed for the real-time RT-PCR. The RNA standard was prepared by *in vitro* transcription. Briefly, the viral genomic region (nt 13918-14246) was amplified by RT-PCR using primer pairs, T7-GP5F (TCTAGATAATACGACTCACTATAGGGAACTTGACGCTATGTGAGCTG, underline indicates T7 promoter) and GP5R (TAGAGTCTGCCCTTAGTGTCCA). PCR product was purified and subjected to *in vitro* transcription using MEGAscript® T7 Transcription Kit (Invitrogen, Carlsbad, CA). The purified RNA product was used as the quantification standard.

Quantitative analysis of mRNA. Porcine alveolar macrophages were infected with WT virus or nsp1β mutants at a MOI of 1. At 12 h post-infection, PAMs were harvested with TRIzol LS (Ambion, Foster City, CA) and subjected to total RNA extraction according to the manufacturer's instruction. After removing contaminating genomic DNA with TURBO DNA-free™ Kit (Invitrogen, Carlsbad, CA), 1μg total RNA was used to synthesize first-strand cDNA using SuperScript® VILO™ cDNA Synthesis Kit (Invitrogen, Carlsbad, CA). Subsequently, real-time PCR was performed to quantify the expression of mRNA of ISG15, IFIT1, IFITM1 and β-tubulin using predesigned primer/probe sets (Applied Biosystems, Foster City, CA), following the manufacturer's instruction. The amount of ISG15, IFIT1 and IFITM1 mRNA was normalized to the endogenous β-tubulin mRNA.

Analysis of swine cytokine response. Porcine alveolar macrophages were infected with WT virus or nsp1β mutants at a MOI of 1. At 12 h post-infection, cell culture supernatant was harvested

for analyzing the IFN-α expression using ProcartaPlex Porcine IFN alpha Simplex kit (eBioscience, San Diego, CA). In addition, Serum, BALF and lung lysate samples were used for measuring the levels of secreted cytokines, IFN-α, IFN-γ, IL-6, and IL-10 by ELISA as described previously (34).

Pig NK cell cytotoxic assay. To determine the pig NK cell-mediated cytotoxicity, the immunofluorescence based assay was performed using a modified method described previously (34-36). The assay was conducted using the 7-AAD/CFSE cell-mediated cytotoxicity assay kit (Cayman Chemical, Ann Arbor, MI). Briefly, PBMCs isolated from pigs were used as the source of NK cells (effectors) against K562 (human myeloblastoid cell line) target cells. The target cells were labeled with CFSE according to the manufacturer's recommendation. Effector and target cells were incubated at different E:T ratios at 37^{o} C overnight. The frequency of apoptotic CFSE-labeled K562 cells that were mediated by NK cells was measured by staining the co-cultured target cells with the 7-AAD nuclear dye. The specific NK cell-cytotoxicity was measured using flow cytometry by acquiring 10,000 CFSE labeled events, and further gated for CFSE and 7ADD (green and red) double staining cell frequency, which indicates the NK-lysed cell frequency. Appropriate controls include K562 cells labeled or unlabeled with CFSE, and apoptosis induced K562 cells (treated with UV at 254nm for 30 min and then incubated for 6-8 h at 37 ^{o}C). The percentage of NK-specific lysis was calculated using the formulae: double positive K562 cells/CFSE positive cells multiplied by 100.

Flow cytometry analysis. Immunophenotyping of PBMCs was performed as previously described (33, 37). Briefly, PBMCs were first surface-labeled with pig lymphocyte specific fluorochrome-conjugated mAbs (CD3ε-PerCP, CD4α-APC and CD8α-FITC). For intracellular IFN-γ staining, GolgiPlug™ (BD Biosciences, San Jose, CA, USA) and Brefeldin A (B7651,

Sigma-Aldrich, St. Louis, MO) were added during the last 12 h of incubation of PBMCs treated with or without the respective virus as a stimulant at a MOI of 1. The surface immunostained cells were fixed with 1% paraformaldehyde and permeabilized with a cell-permeabilization buffer (85.9% deionized water, 11% PBS without Ca^{2+} or Mg^{2+}, 3% formaldehyde solution, and 0.1% saponin) overnight at 4°C. Cells were washed and stained with fluorochrome-conjugated anti-pig IFN-γ or its isotype control mAb (BD Biosciences, East Rutherford, NJ) in 0.1% saponin containing fluorescence-activated cell-sorting (FACS) buffer. Immunostained cells were acquired using the FACS Aria II (BD Biosciences, East Rutherford, NJ) flow cytometer and analyzed using FlowJo (Tree Star, Ashland, OR, USA) software. All specific cell population frequencies were presented as the percentage of lymphocytes in PBMCs.

Statistical analysis. All the data were expressed as the mean of 3 to 9 pigs ± standard error of the mean (SEM). Statistical analyses were performed using one way analysis of variance (ANOVA) followed by post-hoc Tukey's test using GraphPad InStat Prism (software version 5.0) to establish variations between indicated pig groups. Statistical significance was assessed at $P<0.05$ (*), $P<0.01$ (**), $P<0.001$ (***).

RESULTS

Identification of critical residues on GKYLQRRLQ motif for PRRSV nsp1β function

In our previous study (26), we identified a highly conserved GKYLQRRLQ motif in PRRSV nsp1β that is critical for the innate immune suppression function of this protein. Protein structural analysis showed that three basic residues (K124, R128, and R129) in G**K**YLQ**RR**LQ motif are exposed on the surface of nsp1β (25). In this study, we further investigated the function of these three basic residues. A panel of nsp1β mutants was generated. Each of the nsp1β genes

carries a single alanine substitution at amino acid K124 (K124A), R128 (R128A), R129 (R129A) or double alanine substitutions at R128/R129 (RR129AA). A previously created mutant nsp1βKO (R124/R128 to A124/A128 double substitutions (26)) was also included in the analysis. These nsp1β mutants were cloned into the plasmid vector, p3xFLAG-Myc-CMV™-23, in which the gene expression is under the control of CMV promoter and expressed as a 3xFLAG-tagged protein. Initially, this panel of nsp1β mutants was analyzed in an IFN-β promoter driven-luciferase reporter assay. The HEK-293T cells were co-transfected with a plasmid expressing wild type (WT) or mutated nsp1β and a reporter plasmid (p125-Luc) that expresses firefly luciferase reporter gene under the control of IFN-β promoter. The empty vector (EV), p3xFLAG-Myc-CMV™-23, was included in the analysis as a control. At 24 h post-transfection, cells were mock-infected or infected with Sendai virus (SeV). Cells were harvested to test the luciferase activities at 16 h post-infection (hpi). As shown in Figure 1A, SeV infection induced high level of luciferase reporter expression in cells transfected with empty vector, but luciferase expression was about 46 to 16-fold lower in cells expressing WT nsp1β and K124A mutant. In contrast, in comparison to that of WT nsp1β, about 33-fold, 19-fold, 24 fold and 26-fold higher level of reporter signal was detected in cells expressing R128A, R129A, RR129AA and 1βKO mutants, respectively. We further determined whether these mutations had effect on nsp1β's ability to suppress IFN-dependent signaling pathway for the interferon-stimulated genes (ISGs) expression. The panel of nsp1β mutants was analyzed using an ISRE promoter driven-luciferase reporter assay. Similar result was generated as that obtained in Figure 1A, in comparison to that of cells expressing WT nsp1β about 38-fold, 46-fold, 75-fold and 71-fold higher level of reporter signal was detected in cells expressing R128A, R129A, RR129AA and 1βKO mutants, respectively (Figure 1B). These results suggest that R128 and R129 are critical to IFN antagonist

function of nsp1β. In contrast, K124 appeared to be not significantly affecting the IFN antagonist function of nsp1β.

The expression level of nsp1β was evaluated by western blot analysis using mAb M2 against FLAG-tag. The result confirmed the expression of nsp1β in WT and mutants-transfected cells used in luciferase assays (Figure 1C). In our previous study, we showed that double mutations of K124/R128 to A124/A128 caused increased amount of nsp1β expression in comparison to that of WT nsp1β and other mutants, which suggested that nsp1β may suppress its "self-expression" (26). In this study, individual substitutions introduced in K124, R128 and R129 showed that only R128A substitution affects the ability of nsp1β to suppress "self-expression" *in vitro*. The detailed mechanism for nsp1β's ability to suppress "self-expression" and whether such property relates to innate immune suppression function of the virus needs to be further studied (see more details in Discussion section).

We further determined whether mutations introduced in GKYLQRRLQ motif also affect the transactivator function of nsp1β. A vaccinia/T7 polymerase system expressing nsp1β-2 region was used to analyze the expression of nsp2 and PRF products. The expression of -2 PRF product (nsp2TF) was determined by immunoprecipitation (IP) and Western blot (WB). Equal amount of lysates of transfected cells expressing WT nsp1β-2 or its mutants (K124A, R128A, R129A, 1βKO, and RR129AA) were subjected to immunoprecipitation using the polyclonal Ab (pAb-TF) that specifically recognizes the C-terminal peptide of nsp2TF. Subsequently, western blot analysis was performed using pAb-TF and mAb140-68 that recognizes the N-terminal PLP2 domain of the protein. As shown in Figure 2A, the nsp2TF product only detected in cells

337 expressing nsp1β-2 WT or K124A mutant, but not detected in cells expressing R128A, R129A,
338 RR129AA mutants. In contrast, the expression of full-length nsp2 and nsp1β was detected in WT
339 and all mutants of nsp1β-2 (Figure 2B). The result indicates that residue R128 and R129 are
340 critical for the transactivator function of nsp1β in activating -2 PRF. K124 did not show
341 significant effect on the nsp1β function in PRF transactivation.
342
343 ***In vitro* characterization of recombinant viruses containing mutations in GKYLQRRLQ**
344 **motif**

345 To further investigate whether the specific substitutions introduced into the nsp1β
346 GKYLQRRLQ motif of the virus could improve innate immune responses in PRRSV-infected
347 cells, we created a panel of recombinant viruses using reverse genetics. Three viable
348 recombinant viruses were generated, including vSD95-21-R128A (vR128A), vSD95-21-R129A
349 (vR129A) and vSD95-21-R128A/R129A (vRR129AA), carrying single or double mutations at
350 the residue R128 and R129 of the GKYLQRRLQ motif. As a comparison, recombinant viruses
351 with the mutation at K124 (vSD95-21-K124A; vK124A), the double mutations at K124/R128
352 (vSD95-21-K124A/R128A; v1βKO), and the WT virus, vSD95-21 were also recovered from
353 reverse genetics. Stability of those mutations introduced into the virus was determined by serially
354 passaging each virus 5 times in MARC-145 cells, and sequence analysis of passage 3 and
355 passage 5 viruses showed that all of the introduced mutations were stably maintained in the
356 mutant viruses. The growth property of these mutants (passage 3) was compared with the WT
357 parental virus. In comparison to WT virus (peak viral titer of $10^{7.33}$ $TCID_{50}$/ml), vK124A showed
358 similar growth ability, while vR128A and vR129A showed certain levels of reduced growth
359 ability (peak viral titers of $10^{7.0}$ $TCID_{50}$/ml and $10^{6.58}$ $TCID_{50}$/ml, respectively). In contrast,

vRR129AA and v1βKO mutants had significantly reduced growth ability with about 1~1.5 logs decrease in viral titer through the time course of study (Figure 3A). Plaque assay result consistently showed that v1βKO and vRR129AA developed smaller plaques than that of WT virus (Figure 3B).

Expression of innate immune genes in nsp1β mutant virus-infected cells

As we determined that R128A and/or R129A mutations introduced in GKYLQRRLQ motif reduced the nsp1β's ability to suppress innate immune response (Figure 1), we further analyzed whether these mutations could alter the inhibitory effect of PRRSV on type I IFN production and signaling. Since K124A did not show much effect on the function of nsp1β in PRF transactivation and innate immune suppression, recombinant viruses containing K124A substitution (vK124A and v1βKO) were not further analyzed in the following experiments (see Discussion section for more description about the characteristics of v1βKO). Initially, IFN-α expression was evaluated in nsp1β mutants or WT virus-infected porcine alveolar macrophages (PAMs) using ProcartaPlex Porcine IFN alpha Simplex kit (eBioscience, San Diego, CA). PAMs were initially infected with equal amount (MOI=1) of WT or an nsp1β mutant. At 12 h post-infection, IFN-α concentration in the cell culture supernatant of virus-infected porcine alveolar macrophages (PAM) was evaluated. All of the nsp1β mutants showed improved ability to induce the production of IFN-α, which is indicated by 3.3-fold (vR128A), 6.1-fold (vR129A), and 50-fold (vRR129AA) higher concentration of IFN-α in the supernatant of mutant viruses infected cells than that of WT virus infected cells (Figure 4A). Of note, vRR129AA showed the strongest stimulation of IFN-α production. In addition, the expression of nsp1β was detected by western blot, indicating successful viral replication in PAM of WT virus and nsp1β mutants (Figure 4E).

Subsequently, we analyzed whether these mutations could alter the inhibitory effect of PRRSV on the production of ISGs. At 12 h post-infection, the mRNA expression level of three selected ISGs, ISG15, IFIT1 and IFITM1, was assessed via quantitative real-time PCR using predesigned primers/probe sets (Applied Biosystems, Foster city, CA). Consistent with their improved ability for IFN-α induction, all of the nsp1β mutants stimulated higher mRNA expression level of ISGs. As indicated in Figure 4B, in comparison with that of WT virus infected cells, about 4.1-fold (vR128A), 7.8-fold (vR129A) and 20-fold (vRR129AA) higher mRNA expression of ISG15 was detected in mutant viruses infected cells, although the increase in vR128A and vR129A infected cells is not statistically significant. Similarly, the mRNA expression levels of IFIT1 and IFITM1 were increased in mutant viruses infected cells in comparison to that in WT virus infected cells (Figure 4C and 4D).

***In vivo* characterization of nsp1β mutants**

Subsequently, we obtained five groups of 4-week-old pigs to determine whether the R128 and R129-related mutants could improve specific immune responses in PRRSV-infected pigs. As shown in Table 1, each group of pigs (n=9) was infected with the WT virus, an nsp1β mutant, or mock-infected with cell culture medium as negative control. The serum, BALF, and lung lysate samples were collected and stored at -80 ^{o}C for further analysis. We did not observe any noticeable clinical PRRS symptoms and fever in any of the WT virus or nsp1β mutant-infected pigs.

Viral load in serum and tissue samples. Initially, we measured viral RNA load in serum samples using real-time quantitative RT-PCR (qRT-PCR). In comparison with the group of pigs infected

406 with WT virus, pigs infected with vR128A and vRR129AA mutants showed consistently lower
407 viral RNA load through the entire time course of the experiment, while pigs infected with
408 vR129A mutant exhibited lower viral RNA load from 1 DPI to14 DPI (Figure 5A). In pigs
409 infected with the vR128A mutant, statistically significant lower level of viral RNA load was
410 obtained at 1, 2, 5, and 14 DPI, in comparison to that in pigs infected with WT virus (Figure 5A).
411 At most of the time-points, especially at the later stage of the infection, the mean viral RNA load
412 in pigs infected with vRR129AA mutant was the lowest among all the infected pigs (Figure 5A).
413 Surprisingly, vR129A mutant infected pigs showed similar level of mean viral RNA load as the
414 group of pigs infected with WT virus at 21 DPI, and exhibited higher (but not statistically
415 significant) viral RNA load than that of pigs infected with WT virus at 28 DPI and 35 DPI.

416 Since qRT-PCR does not distinguish between viable and nonviable forms of the virus, we further
417 quantified infectious virus particles in serum samples. Infectious virus titer was measured
418 through micro-titration assay using MARC-145 cells. At 1, 2 and 5 DPI, infectious viral titers in
419 groups of pigs infected with nsp1β mutants were about 1~3 log lower (statistically significant)
420 than the viral titers in pigs infected with WT virus (Figure 5B), which is consistent with viral
421 loads quantified by qRT-PCR (Figure 5A). The infectious viral titer in many pigs infected with
422 nsp1β mutants was lower than the detection limit ($10^{1.67}$ $TCID_{50}$/ml) of the micro-titration assay
423 through the time course of infection. The rebounded viral titer was observed in vR129A mutant-
424 infected pigs at 21, 28 and 35 DPI, which is consistent with the viral RNA load data generated by
425 qRT-PCR. These results indicate that the growth ability of vR128A and vRR129AA was
426 attenuated *in vivo,* and the growth ability of vR129A was attenuated at early stage of infection
427 but reverted to WT phenotype at certain level during the later stage of infection (see sequencing
428 data in Table 2).

Since PAM serves as the primary target cell for PRRSV, we further evaluated the viral load in lung lysate and BALF collected at 7, 21 and 35 DPI. Viral RNA load was quantified by qRT-PCR and infectious viral titer was determined by micro-titration assay. Results from both qRT-PCR and micro-titration assay showed that the viral loads in lung and BALF from all groups of pigs infected with nsp1β mutants were consistently lower than that in pigs infected with WT virus at 7 and 21 DPI (Figure 6), although some of the differences were not statistically significant. At 35 DPI, the lower level of mean viral load and infectious viral titer were detected in lung samples from pigs infected with vR128A and vRR129AA mutants, in comparison with that in pigs infected with WT virus (Figure 6). In the lung samples from vR129A mutant infected pigs, the mean viral load and infectious viral titer were reached similar level as that of WT virus-infected pigs at 35 DPI. These results suggest that nsp1β mutants have attenuated replication ability in the lung of infected pigs, but vR129A showed reversion to WT phenotype at certain level during later stage of infection.

Genetic stability of nsp1β mutants in pigs. The genetic stability is one of the important criteria for selecting vaccine candidates. Initially, serum samples from 3 pigs per group terminated at 21 DPI were used to determine the stability of the introduced mutations. The nsp1β coding region was RT-PCR amplified and the PCR product was subjected to DNA sequencing analysis. As showed in Table 2, no 2nd site mutation and also no reversion were found in nsp1β coding region of the virus that isolated from serum samples of the pigs infected by vRR129AA mutant virus. In the group of pigs infected with vR128A mutant, the designed mutation was maintained in the viruses recovered from all three tested pigs, but several 2nd site mutations were observed, including the substitution of Asp^{9} to Gly and Ser^{122} to Pro in all three pigs, and His^{109} and Leu^{141} substituted by Arg and Pro in one pig, respectively. In the group of pigs infected with vR129A

452 mutant, the designed mutation in one of the three tested pigs reversed from Ala back to Arg (in
453 WT virus), and R129A was maintained in the other two pigs. Similar to vR128A group, 2nd site
454 mutation, Ser122 to Pro, was detected in those two pigs that maintained designed mutation; an
455 additional mutation of Ser169 to Pro occurred in one of the two pigs, and the substitution of Asp9
456 to Gly was observed in all three pigs. Since there was a reversion occurred in one of the vR129A
457 mutant-infected pig at 21 DPI, we further analyzed serum samples from all 6 pigs infected with
458 vR129A at 14 DPI. Remarkably, the pig with Ala129 to Arg reversion at 21 DPI had already
459 obtained the reversion at 14 DPI. However, the designed R129A mutation was maintained in all
460 other five pigs. It is worth noting that the 2nd site substitution of Ser122 to Pro occurred in all of
461 the pigs that maintained designed mutations (R128A and R129A) at 14, 21 and 35 DPI,
462 suggesting that this substitution may compromise the effect of designed mutations on viral
463 growth ability in *vivo*. Interestingly, the mutation of Asp9 to Gly was not only detected in pigs
464 infected with all mutants, but also observed in pigs infected with WT virus. This mutation may
465 relate to the *in vivo* fitness of PRRSV, which was most likely not caused by our designed
466 mutations. In addition, using the serum samples at 35 DPI that was determined to be PRRSV
467 RNA positive by real-time RT-PCR, no reversion was observed in sequencing analysis. We
468 searched PRRSV full-length genome sequences available in the Genbank (as of 7/27/2015), all
469 of the 2nd site substitutions that observed here are able to be found in field strains, for example,
470 PRRSV P129 strain contains Pro122. Taken together, among the three nsp1β mutants, vRR129AA
471 maintained the best genetic stability *in vivo* with no reversion and less 2nd site mutation detected
472 in nsp1β-coding region.

473 ***Innate immune response in PRRSV nsp1β mutants infected pigs.*** To determine whether the
474 mutations introduced into nsp1β region could improve PRRSV-specific innate immune response,

we initially measured IFN-α expression in infected and control pigs during the early stage of infection. Compared to WT virus-infected pigs, a 1.5-fold higher (but was not significant) levels of IFN-α was observed in serum samples of vRR129AA infected pigs at 1 DPI (data not shown). Since the virus replicates primarily in alveolar macrophages and we inoculated the virus by intranasal (IN) route, the immune response in the lung is important, we measured IFN-α levels in both BALF (represents airways) and lung lysate (represents lung parenchyma, local site of PRRSV infection). In the BALF at 7 DPI, the IFN-α was comparable among all pig groups, while at 21 and 35 DPI in pigs inoculated with vRR129AA and vR129A mutant viruses, there was an increased level (but not statistically significant) of IFN-α production compared to that of WT virus-infected pigs (data not shown). At 7 DPI, in the lung lysate of pigs inoculated with nsp1β mutant viruses, higher levels of IFN-α were observed compared to that of WT virus-infected pigs (Figure 7A).

IFN-α is critical for natural killer (NK) cell-mediated cytotoxic function. To determine whether the nsp1β mutations impaired IFN-α antagonist function of the virus, PBMCs from mutants and WT virus-infected pigs were used as a source of NK cells to evaluate NK cell function in the NK cell-cytotoxicity assay. At both the E:T ratios (100:1 and 50:1), the vRR129AA mutant virus-infected pigs had increased activity of NK cell cytotoxic function at 7 DPI (Figure 7B and C). This result is consistent with the increased level of IFN-α production in the serum and lung lysate of vRR129AA-infected pigs.

Adaptive immune response in PRRSV nsp1β mutants infected pigs. A strong innate immune response following a virus infection augments the cell-mediated adaptive immunity. Therefore, we analyzed the production of an important Th1 cytokine IFN-γ response in WT virus and nsp1β

497 mutants-infected pigs. The production of IFN-γ in the serum of WT virus-infected pigs was
498 undetectable throughout the time course of the study (0-35 DPI), while in the serum of nsp1β
499 mutants-infected pigs, spurts of IFN-γ secretion (100-150 pg/ml) was detected at multiple DPIs,
500 with IFN-γ detected from vR129A mutant-infected pigs at 7-21 DPI, and IFN-γ detected from
501 vRR129AA mutant infected pigs at 14 and 28 DPI (Figure 8A). In vR128A mutant-infected pigs,
502 increased IFN-γ in serum was detected at 5 and 14 DPI (Figure 8A). Such an early response of
503 IFN-γ in nsp1β mutants-infected pigs might be due to the rescue of adaptive immunity mediated
504 through induction of IFN-α secretion and NK cell function by these mutants. A similar increase
505 in IFN-γ secretion (but not statistically significant) was detected in the BALF of vR128A,
506 vR129A and vRR129AA infected pigs, observed at only 7 DPI (data not shown). However, an
507 increased level of IFN-γ production in the lung lysate of vR129A and vRR129AA infected pigs
508 at 7 DPI was significantly higher than that of WT virus-infected pigs (Figure 8B).

509 Production of the pro-inflammatory cytokine IL-6 suggests the inflammatory reaction in the
510 lungs of pigs (34). The levels of IL-6 was higher (but not significant) at 21 DPI in the BALF of
511 vR129A and vRR129AA infected pigs compared to that of WT virus infected pigs (Figure 8C).
512 In the lung lysate of vRR129AA infected pig at 21 DPI, a significantly higher level of IL-6
513 production was detected compared to that of WT virus infected pigs (Figure 8D). This data
514 suggests that the induction of IL-6 production by the vRR129AA mutant virus in pigs appears to
515 be responsible for augmenting the IFN-γ production, an indicator of adaptive immunity.

516 We further evaluated the frequency of different T cell subpopulation in PBMCs, expressed as the
517 percentage of $CD3^+$ or $CD3^-$ cells. The pig T cells expressing the combination of phenotypic
518 markers $CD3^+CD4^-CD8\alpha^+$ are either cytotoxic T cells (CTLs) or γδ T cells, and cells with

519 $CD3^+CD4^-CD8\alpha\beta^+$ are exclusively CTLs (38, 39). Porcine immune system has a unique
520 frequency of $CD3^+CD4^+CD8\alpha^+$ T cells, which have the memory, cytotoxic, and T-helper cell
521 properties (40, 41). To determine antigen specific activation of T cell response, IFN-γ secreting
522 lymphocyte subsets were elucidated by re-stimulating PBMCs with the same virus *in vitro*. In
523 every phenotypic marker staining, respective isotype controls were included to eliminate the
524 background. The specific population of cells was identified based on combination of phenotypic
525 cell surface markers, which include $CD3^+CD4^-CD8\alpha^+$ (CTLs or γδ T cells), $CD3^+CD4^+CD8\alpha^+$
526 (T-helper/memory), and $CD3^-CD4^-CD8\alpha^+$ (NK) cells (38, 40-43). Subsequently, the cells were
527 fixed and stained for intracellular IFN-γ and gated for their respective activated ($IFN\text{-}\gamma^+$)
528 phenotype. Frequency of total CTLs/γδ T cells in vR129A and vRR129AA infected pigs were
529 numerically increased (but not statistically significant) at 21 DPI and were significantly reduced
530 at 35 DPI compared to WT virus infected pigs (Figure 9A), while the activated ($IFN\text{-}\gamma^+$)
531 CTLs/γδ T cells in the same mutants infected pigs were numerically increased and decreased
532 (but not statistically significant) compared to WT virus at DPI 7 and 35, respectively (Figure
533 9B). In comparison of WT virus-infected pigs with vR129A and vRR129AA-infected pigs,
534 exactly a similar trend (but not statistically significant) in total and activated T-helper/memory
535 cell frequencies to that of CTLs/γδ T cells was observed at all three DPIs (Figure 9C and D). The
536 frequency of NK cells was significantly increased only in vRR129AA infected pigs at 7 DPI
537 (Figure 9E). This data suggest that the NK cells and the two important T cell subsets were
538 activated particularly in vRR129AA mutant PRRSV-infected pigs, suggesting the virus specific
539 activation of innate and adaptive immunity.
540
541

DISCUSSION

Many studies have demonstrated that a potent innate immune response induced by microbial infection / vaccination will lead to generation of sufficient adaptive immunity, which subsequently clears the pathogen infection from the host completely (44, 45). However, PRRSV infection generally induces poor anti-viral innate IFN and cytokine responses, which results in weak adaptive immunity (46-50). One of the key steps in new PRRS vaccine construction is to develop strategies to target these initial immune response events to enhance the viral specific immunity. Previous studies for other viral pathogens showed that recombinant viruses generated with targeted mutations (deletions) in genes encoding for immune antagonists are excellent candidates for MLV vaccines (51-54). The (selected) recombinant viruses normally grow well in tissue culture; while in infected animals, they are attenuated but still replicate to sufficient amounts for stimulating robust immune responses. Several PRRSV proteins have been identified as antagonists to the type I IFN induction (and signaling), and nsp1β was determined having the strongest inhibitory effect among those proteins (22-24, 26). Therefore, in this study, our vaccine development strategy is to generate recombinant viruses with targeted mutations in the nsp1β regions.

Our previous study identified a highly conserved GKYLQRRLQ motif in nsp1β that is critical for its inhibitory effect on type I IFN production and signaling. Based on the crystal structure of nsp1β, three basic residues (K124, R128, and R129) in G**K**YLQ**RR**LQ motif are exposed on the surface of the protein. In our previous study, double mutations of K124A/R128A impaired the IFN antagonist function of nsp1β (26). In this study, we further tested each of these three individual residues. In comparison to WT nsp1β, nsp1β mutants carrying alanine substitution at R128 and R129 showed a significantly reduced antagonism effect on reporter gene expression

565 under the control of IFN-β promoter (p125-Luc); however, K124A mutant still had a similar
566 inhibitory effect on reporter gene expression as that of WT nsp1β. Similar results were observed
567 in the luciferase reporter assay (pISRE-Luc) utilized to examine the inhibitory effect on type 1
568 IFN signaling. Both the WT nsp1β and K124A mutant severely suppressed luciferase reporter
569 expression, in contrast to significant higher level of luciferase expression in cells transfected with
570 nsp1β mutants that contain mutations at R128 and/or R129 (Figure 1B). These results indicate
571 that R128 and R129 residues, but not K124, are critical for nsp1β's function in antagonizing type
572 1 IFN production and signaling.

573 As we discussed previously (26), suppressing host cellular gene expression, including nsp1β
574 "self-expression" could be a mechanism of its immune antagonist function. Compared to the
575 expression level of WT nsp1β, obviously higher level of nsp1β expression was detected in
576 western blot analysis for R128A and K124A/R128A (1βKO) mutants (Figure 1C). Interestingly,
577 when R129A substitution combines with R128A (RR129AA), it appeared to restore the nsp1β's
578 ability to suppress its "self-expression". The single alanine substitution of R129 residue did not
579 impair the ability of nsp1β to suppress its "self-expression", although it attenuated nsp1β's
580 ability to suppress type I IFN expression. These data make us speculate that different
581 mechanisms may be utilized by R128 and R129 residues to evade host innate immune defense,
582 which needs to be further elucidated.

583 As we discussed above, besides function as an innate immune antagonist, nsp1β was recently
584 identified as a transactivator for the expression of -2/-1 PRF products, nsp2TF and nsp2N. Both
585 nsp2TF and nsp2N share the N-terminal 2/3 sequence with nsp2, which contains the PLP2
586 domain. PLP2 was also identified as an innate immune antagonist that is capable of removing
587 ubiquitin (Ub) and Ub-like modifiers like ISG15 from host cell substrates (55-58). When testing

the nsp1β effect during viral infection (see below), it remains to be established to what extent nsp1β directly modulates the innate immune response or does so by stimulating the expression of nsp2TF and nsp2N.

In this study, we generated recombinant viruses of nsp1β mutants using reverse genetics, including vK124A, vR128A, vR129A and vRR129AA. As a comparison, our previously constructed mutant v1βKO (containing double mutations of K124A/R128A) was included in viral growth characterization in cell culture. In comparison to WT virus, all nsp1β mutants except vK124A had attenuated growth ability in cell culture, but their peak viral titers were all reached above 5 logs $TCID_{50}$/mL, which is acceptable for subsequently application in animals. Multiple-step viral growth curves showed that vR128A and vR129A had slightly slower growth kinetics, while v1βKO and vRR129AA showed 1~1.5 logs lower virus titer than that of parental virus at all the tested time points (Figure 3A). It is worth noting that v1βKO containing the double mutations of K124A/R128A had lower virus titer than that of mutant virus with single mutation of R128A, but single K124A mutation did not affect much on the virus growth ability in cell culture. In addition, none of the mutations affected the release of nsp1β from nsp1β-2 polyprotein (Figure 2B), suggesting that the reduced growth rate (viral titer) of the nsp1β mutants may not directly caused by a basic defect in replicase polyprotein proteolysis. We speculate that R128A, R129A, or combined K124A/R128A, and R128A/R129A mutations may change nsp1β protein or RNA structure, which in turn affects virus replication ability. The in depth mechanism of these mutations that affects viral growth ability requires more studies in the future. When tested in the vaccinia/T7 expression system, the expression of nsp2TF was impaired by alanine substitutions at residue 128 and 129 using nsp1β-2 expression constructs (Figure 2A). Under the virus infection condition, these two residues are also essential for the

PRF transactivator function of nsp1β (data not shown). Taken together, our data indicate that the three basic amino acids exposed on nsp1β surface appear to have different functions, and the detailed mechanism needs to be further elucidated.

Subsequently, these mutants were characterized in nursery pigs. Since the K124A did not have much effect on innate suppression function of nsp1β, and the recombinant virus containing K124A mutation did not affect much on viral replication, this mutant was excluded in current animal study. In a previous study, we evaluated 1βKO and WT viruses in pigs. The 1βKO showed over-attenuated phenotype with virus grew in extremely low titer (~ $5x10^4$ RNA copies/ml in serum), which is 2 to 3 logs lower than that of wild type virus. As a consequence, pigs did not seroconvert until 28 dpi. The initial IFN-α response was very limited (8.4 pg/mL serum at 3 DPI); in contrast, we could detect certain level of IFN-α response (100.9 pg/mL serum at 3 DPI) in WT virus-infected pigs. As we discussed above, single mutation on K124 residue did not seem to affect much on the *in vitro* growth ability of the virus, but combined mutations with R128 significantly impaired the virus growth ability *in vitro* and *in vivo*. The in depth mechanism of K124 involved in viral replication and its function in relation to combined effect of R128 mutation need to be further studied. Since our previous data showed over-attenuated phenotype of 1βKO, in the current study, we focused on characterizing the other three nsp1β mutants (vR128A, vR129A, and vRR129AA) in nursery pigs. Active virus replication was observed in all of the virus-infected pigs. The viremia data indicate that, in consistent with *in vitro* results, nsp1β mutants were also attenuated in pigs. At all the time-points, in comparison to WT virus-infected pigs, vR128A- and vRR129AA-infected pigs had consistently lower levels of mean viral RNA load and infectious virus titer. For vR129A group, these pigs also had lower levels of viremia than that of WT virus group at the early time-points; however, they showed

even higher level of viremia than that of WT group at 35 DPI. These results suggest that the virus in vR129A could be reversed back to WT virus. Subsequently, sequence analysis of nsp1β coding region was performed to confirm the stability of the mutations introduced into the virus. From viruses recovered at 21 DPI, the designed alanine substitutions were stably maintained, except a reversion identified in one of the pigs (pig #31) infected with vR129A. We further sequenced nsp1β coding region in the viruses recovered from vR129A infected pigs at 14 DPI, the result showed that the reversion only occurred in pig #31, but not the other five tested pigs. Unexpectedly, no reversion in the nsp1β coding region was identified in vR129A group of pigs at 35 DPI, although vR129A group of pigs showed even higher virus titer than that of WT group of pigs. We speculate that the spontaneous mutations in other regions of viral genome may compensate viral replication ability in *vivo*. Remarkably, for those viruses stably maintained the designed mutations vR128A and vR129A in infected pigs, a specific 2nd site mutation of Ser^{122} to Pro^{122} was consistently identified. We analyzed the sequence of nsp1β from *in vitro* expression plasmids and original recombinant viruses that grew in MARC-145 cells (before inoculation into pigs), and the result showed that Ser^{122} was stably maintained in vR128A, vR129A and vRR129AA. The data suggest that Pro^{122} may contribute the viral fitness *in vivo* and Ser^{122} to Pro^{122} substitution may compromise the side effect of our designed mutations on virus replication ability in animals. Whether the Ser^{122} to Pro^{122} substitution has effect on the function of nsp1β needs to be further studied.

Given the impaired ability of nsp1β mutants vR128A, vR129A and vRR129AA to antagonize innate immune response *in vitro*, we further assessed the ability of these viruses in the induction of host immune response *in vivo*. After immunization, no clinical symptoms and adverse side effects were observed in the WT and mutant virus-infected pigs. In addition, when terminated

three pigs per group at 7, 21 and 35 DPI, no obvious lung lesion was observed. This result is expected, since the WT virus SD95-21 (backbone of nsp1β mutants) has 99.5% nucleotide identity with that of VR2332, the parental virus of PRRS modified live virus (MLV) vaccine (Ingelvac PRRS MLV; Boehringer Ingelheim Vetmedica, Inc.), and 99.6% identity to Ingelvac PRRS MLV. In addition, SD 95-21 virus was adapted growth in MARC-145 cells. In previous studies, pigs infected with PRRS MLV strain of VR2332 showed very mild or undetectable clinical, gross and histopathological lesions (59). The goal of our vaccine development is to improve the ability of current MLV vaccine to stimulate higher innate and cell mediated immune responses.

Since type 1 IFNs are the principle cytokines for innate immunity against viral infections, IFN-α was selected as a representative to assess the ability of PRRSV to induce host innate immune response. In consistent with our data generated in *in vitro* expression system, nsp1β mutants induced higher level of IFN-α than that of WT virus during early time period post-infection. In comparison to that of WT virus infected pigs, higher cytotoxic activity of NK cells was also observed in pigs infected with nsp1β mutants. These results suggest that PRRSV nsp1β plays a crucial role in suppressing host innate immunity, and modifying this protein could effectively improve the ability of PRRSV to stimulate host innate immune response. Furthermore, these mutants induced earlier and higher level of IFN-γ expression compared to WT virus. As an important factor in adaptive immunity against viral infection, IFN-γ increases antigen presentation and promotes Th1 cell differentiation (60). The increased expression of IFN-γ in mutant viruses infected pigs indirectly indicates the activation of Th1 cell-mediated immune response. This was observed not only in serum of mutants infected pigs, but also indicated by increased activation of CTLs/γδ T, T-helper/memory, and NK cells. Previously, increased

680 frequency of activated T-helper/memory cells in pigs was shown to be beneficial in virus
681 clearance in Aujeszky's disease virus, African and Classical swine fever virus, and PRRSV
682 infections (33, 41, 61-64). Taken together, besides induction of higher level innate immune
683 response, these mutants may also have stronger ability in augmenting Th1 cell-medicated
684 adaptive immunity in comparison to that of WT virus. As a candidate vaccine, one would expect
685 its ability to stimulate significant humoral response in animals. In fact, we performed both
686 neutralizing antibody and ELISA assays using serum samples, but the result showed no
687 significant difference among pig groups infected with WT virus and three nsp1β mutants (data
688 not shown). It is a well-established phenomenon that strong Th1 response suppresses the Th2
689 response (humoral response) and vice-versa, which were demonstrated previously in mice (65,
690 66) and pigs (33, 64, 67). Therefore, our data suggest that lack of improved virus neutralizing
691 antibody response in nsp1β mutants-infected pigs could be caused by the strong Th1 response.
692 Future virus challenge study in the nsp1β mutant vaccinated pigs may reveal benefits of
693 increased Th1 response in viral clearance.

694 Based on our data, the nsp1β mutant, vRR129AA, could be a potential vaccine candidate, and
695 this attenuation strategy could be easily applied to improve current vaccines. This conclusion is
696 based on multiple observations. First, vRR129AA can grow to sufficient virus titers in cell
697 culture (greater than 5 log $TCID_{50}$/mL), which facilitate large scale vaccine production. Second,
698 in comparison to WT virus, vRR129AA induced earlier and stronger innate immune response,
699 which was supported by elevated IFN-α expression and NK cell cytotoxic activity. The improved
700 innate immune response appears to augment cell-mediated adaptive immunity, indicated by early
701 induction of IFN-γ expression by both NK cells and T cells, followed by depletion of activated T
702 cell subsets as presented in phenotypic analysis of PBMCs. Another important aspect is that this

mutant appeared to be quickly cleared from virus-infected pigs, and showed better genetic stability than nsp1β mutants containing single alanine substitution (vR128A, vR129A). Nevertheless, the protection efficacy of this potential vaccine candidate needs to be further assessed in animal challenge study. Finally, R128 and R129 residues are highly conserved in all available PRRSV strains as described previously (25, 26), in which the technology described in this study can be easily applied to current commercial vaccines and other candidate vaccines.

ACKNOWLEDGEMENTS

We thank Professor Eric J. Snijder (Leiden University Medical Center, Leiden, The Netherlands) for helpful discussion, Russell Ransburgh and Elizabeth Poulsen (Kansas State University, Manhattan, KS, USA) for technical assistance. This project was supported by Agriculture and Food Research Initiative Competitive Grant no. 2012-67015-21823 from the USDA National Institute of Food and Agriculture; Kansas State University research startup fund.

716 **REFERENCES**

717 1. **Keffaber KK.** 1989. Reproductive failure of unknown etiology. Am. Assoc. SwinePract.
718 Newsl.**:**1-9.
719 2. **Wensvoort G, Terpstra C, Pol JM, ter Laak EA, Bloemraad M, de Kluyver EP,**
720 **Kragten C, van Buiten L, den Besten A, Wagenaar F, et al.** 1991. Mystery swine
721 disease in The Netherlands: the isolation of Lelystad virus. Vet Q **13:**121-130.
722 3. **Benfield DA, Nelson E, Collins JE, Harris L, Goyal SM, Robison D, Christianson**
723 **WT, Morrison RB, Gorcyca D, Chladek D.** 1992. Characterization of swine infertility
724 and respiratory syndrome (SIRS) virus (isolate ATCC VR-2332). J Vet Diagn Invest
725 **4:**127-133.
726 4. **Collins JE, Benfield DA, Christianson WT, Harris L, Hennings JC, Shaw DP, Goyal**
727 **SM, McCullough S, Morrison RB, Joo HS, et al.** 1992. Isolation of swine infertility
728 and respiratory syndrome virus (isolate ATCC VR-2332) in North America and
729 experimental reproduction of the disease in gnotobiotic pigs. J Vet Diagn Invest **4:**117-
730 126.
731 5. **Albina E, Madec F, Cariolet R, Torrison J.** 1994. Immune response and persistence of
732 the porcine reproductive and respiratory syndrome virus in infected pigs and farm units.
733 Vet Rec **134:**567-573.
734 6. **Dwivedi V, Manickam C, Binjawadagi B, Linhares D, Murtaugh MP,**
735 **Renukaradhya GJ.** 2012. Evaluation of immune responses to porcine reproductive and
736 respiratory syndrome virus in pigs during early stage of infection under farm conditions.
737 Virol J **9:**45.
738 7. **Murtaugh MP, Xiao Z, Zuckermann F.** 2002. Immunological responses of swine to
739 porcine reproductive and respiratory syndrome virus infection. Viral Immunol **15:**533-
740 547.
741 8. **Renukaradhya GJ, Dwivedi V, Manickam C, Binjawadagi B, Benfield D.** 2012.
742 Mucosal vaccines to prevent porcine reproductive and respiratory syndrome: a new
743 perspective. Anim Health Res Rev **13:**21-37.
744 9. **Snijder EJ, Kikkert M, Fang Y.** 2013. Arterivirus molecular biology and pathogenesis.
745 J Gen Virol **94:**2141-2163.
746 10. **Meulenberg JJ, Petersen-den Besten A, De Kluyver EP, Moormann RJ, Schaaper**
747 **WM, Wensvoort G.** 1995. Characterization of proteins encoded by ORFs 2 to 7 of
748 Lelystad virus. Virology **206:**155-163.
749 11. **Meulenberg JJ, Petersen-den Besten A, de Kluyver EP, Moormann RJ, Schaaper**
750 **WM, Wensvoort G.** 1995. Characterization of structural proteins of Lelystad virus. Adv
751 Exp Med Biol **380:**271-276.
752 12. **Mounir S, Mardassi H, Dea S.** 1995. Identification and characterization of the porcine
753 reproductive and respiratory virus ORFs 7, 5 and 4 products. Adv Exp Med Biol
754 **380:**317-320.
755 13. **Bautista EM, Meulenberg JJ, Choi CS, Molitor TW.** 1996. Structural polypeptides of
756 the American (VR-2332) strain of porcine reproductive and respiratory syndrome virus.
757 Arch Virol **141:**1357-1365.
758 14. **Mardassi H, Massie B, Dea S.** 1996. Intracellular synthesis, processing, and transport of
759 proteins encoded by ORFs 5 to 7 of porcine reproductive and respiratory syndrome virus.
760 Virology **221:**98-112.

15. **Meng XJ, Paul PS, Morozov I, Halbur PG.** 1996. A nested set of six or seven subgenomic mRNAs is formed in cells infected with different isolates of porcine reproductive and respiratory syndrome virus. J Gen Virol **77 (Pt 6):**1265-1270.
16. **Meulenberg JJ, Petersen-den Besten A.** 1996. Identification and characterization of a sixth structural protein of Lelystad virus: the glycoprotein GP2 encoded by ORF2 is incorporated in virus particles. Virology **225:**44-51.
17. **Snijder EJ, van Tol H, Pedersen KW, Raamsman MJ, de Vries AA.** 1999. Identification of a novel structural protein of arteriviruses. J Virol **73:**6335-6345.
18. **Wu WH, Fang Y, Farwell R, Steffen-Bien M, Rowland RR, Christopher-Hennings J, Nelson EA.** 2001. A 10-kDa structural protein of porcine reproductive and respiratory syndrome virus encoded by ORF2b. Virology **287:**183-191.
19. **Johnson CR, Griggs TF, Gnanandarajah J, Murtaugh MP.** 2011. Novel structural protein in porcine reproductive and respiratory syndrome virus encoded by an alternative ORF5 present in all arteriviruses. J Gen Virol **92:**1107-1116.
20. **Li Y, Tas A, Sun Z, Snijder EJ, Fang Y.** 2014. Proteolytic processing of the porcine reproductive and respiratory syndrome virus replicase. Virus Res.
21. **Fang Y, Treffers EE, Li Y, Tas A, Sun Z, van der Meer Y, de Ru AH, van Veelen PA, Atkins JF, Snijder EJ, Firth AE.** 2012. Efficient -2 frameshifting by mammalian ribosomes to synthesize an additional arterivirus protein. Proc Natl Acad Sci U S A **109:**E2920-2928.
22. **Chen Z, Lawson S, Sun Z, Zhou X, Guan X, Christopher-Hennings J, Nelson EA, Fang Y.** 2010. Identification of two auto-cleavage products of nonstructural protein 1 (nsp1) in porcine reproductive and respiratory syndrome virus infected cells: nsp1 function as interferon antagonist. Virology **398:**87-97.
23. **Beura LK, Sarkar SN, Kwon B, Subramaniam S, Jones C, Pattnaik AK, Osorio FA.** 2010. Porcine reproductive and respiratory syndrome virus nonstructural protein 1beta modulates host innate immune response by antagonizing IRF3 activation. J Virol **84:**1574-1584.
24. **Kim O, Sun Y, Lai FW, Song C, Yoo D.** 2010. Modulation of type I interferon induction by porcine reproductive and respiratory syndrome virus and degradation of CREB-binding protein by non-structural protein 1 in MARC-145 and HeLa cells. Virology **402:**315-326.
25. **Li Y, Treffers EE, Napthine S, Tas A, Zhu L, Sun Z, Bell S, Mark BL, van Veelen PA, van Hemert MJ, Firth AE, Brierley I, Snijder EJ, Fang Y.** 2014. Transactivation of programmed ribosomal frameshifting by a viral protein. Proc Natl Acad Sci U S A **111:**E2172-2181.
26. **Li Y, Zhu L, Lawson SR, Fang Y.** 2013. Targeted mutations in a highly conserved motif of the nsp1beta protein impair the interferon antagonizing activity of porcine reproductive and respiratory syndrome virus. J Gen Virol **94:**1972-1983.
27. **Zeman D, Neiger R, Yaeger M, Nelson E, Benfield D, Leslie-Steen P, Thomson J, Miskimins D, Daly R, Minehart M.** 1993. Laboratory investigation of PRRS virus infection in three swine herds. J Vet Diagn Invest **5:**522-528.
28. **Fuerst TR, Niles EG, Studier FW, Moss B.** 1986. Eukaryotic transient-expression system based on recombinant vaccinia virus that synthesizes bacteriophage T7 RNA polymerase. Proc Natl Acad Sci U S A **83:**8122-8126.

29. **Nelson EA, Christopher-Hennings J, Drew T, Wensvoort G, Collins JE, Benfield DA.** 1993. Differentiation of U.S. and European isolates of porcine reproductive and respiratory syndrome virus by monoclonal antibodies. J Clin Microbiol **31:**3184-3189.
30. **Reed LJ, Muench H.** 1938. A simple method of estimating fifty per cent endpoints. American journal of epidemiology **27:**493-497.
31. **Fang Y, Rowland RR, Roof M, Lunney JK, Christopher-Hennings J, Nelson EA.** 2006. A full-length cDNA infectious clone of North American type 1 porcine reproductive and respiratory syndrome virus: expression of green fluorescent protein in the Nsp2 region. J Virol **80:**11447-11455.
32. **Halbur PG, Paul PS, Frey ML, Landgraf J, Eernisse K, Meng XJ, Lum MA, Andrews JJ, Rathje JA.** 1995. Comparison of the pathogenicity of two US porcine reproductive and respiratory syndrome virus isolates with that of the Lelystad virus. Vet Pathol **32:**648-660.
33. **Binjawadagi B, Dwivedi V, Manickam C, Ouyang K, Torrelles JB, Renukaradhya GJ.** 2014. An innovative approach to induce cross-protective immunity against porcine reproductive and respiratory syndrome virus in the lungs of pigs through adjuvanted nanotechnology-based vaccination. Int J Nanomedicine **9:**1519-1535.
34. **Renukaradhya GJ, Alekseev K, Jung K, Fang Y, Saif LJ.** 2010. Porcine reproductive and respiratory syndrome virus-induced immunosuppression exacerbates the inflammatory response to porcine respiratory coronavirus in pigs. Viral Immunol **23:**457-466.
35. **Garcia-Iglesias T, Del Toro-Arreola A, Albarran-Somoza B, Del Toro-Arreola S, Sanchez-Hernandez PE, Ramirez-Duenas MG, Balderas-Pena LM, Bravo-Cuellar A, Ortiz-Lazareno PC, Daneri-Navarro A.** 2009. Low NKp30, NKp46 and NKG2D expression and reduced cytotoxic activity on NK cells in cervical cancer and precursor lesions. BMC Cancer **9:**186.
36. **Lecoeur H, Fevrier M, Garcia S, Riviere Y, Gougeon ML.** 2001. A novel flow cytometric assay for quantitation and multiparametric characterization of cell-mediated cytotoxicity. J Immunol Methods **253:**177-187.
37. **Dwivedi V, Manickam C, Patterson R, Dodson K, Murtaugh M, Torrelles JB, Schlesinger LS, Renukaradhya GJ.** 2011. Cross-protective immunity to porcine reproductive and respiratory syndrome virus by intranasal delivery of a live virus vaccine with a potent adjuvant. Vaccine **29:**4058-4066.
38. **Talker SC, Kaser T, Reutner K, Sedlak C, Mair KH, Koinig H, Graage R, Viehmann M, Klingler E, Ladinig A, Ritzmann M, Saalmuller A, Gerner W.** 2013. Phenotypic maturation of porcine NK- and T-cell subsets. Dev Comp Immunol **40:**51-68.
39. **Sinkora M, Butler JE.** 2009. The ontogeny of the porcine immune system. Dev Comp Immunol **33:**273-283.
40. **Zuckermann FA, Husmann RJ.** 1996. Functional and phenotypic analysis of porcine peripheral blood CD4/CD8 double-positive T cells. Immunology **87:**500-512.
41. **Denyer MS, Wileman TE, Stirling CM, Zuber B, Takamatsu HH.** 2006. Perforin expression can define CD8 positive lymphocyte subsets in pigs allowing phenotypic and functional analysis of natural killer, cytotoxic T, natural killer T and MHC un-restricted cytotoxic T-cells. Vet Immunol Immunopathol **110:**279-292.
42. **Costers S, Lefebvre DJ, Goddeeris B, Delputte PL, Nauwynck HJ.** 2009. Functional impairment of PRRSV-specific peripheral CD3+CD8high cells. Vet Res **40:**46.

43. **Dwivedi V, Manickam C, Patterson R, Dodson K, Weeman M, Renukaradhya GJ.** 2011. Intranasal delivery of whole cell lysate of Mycobacterium tuberculosis induces protective immune responses to a modified live porcine reproductive and respiratory syndrome virus vaccine in pigs. Vaccine **29:**4067-4076.

44. **Kamijuku H, Nagata Y, Jiang X, Ichinohe T, Tashiro T, Mori K, Taniguchi M, Hase K, Ohno H, Shimaoka T, Yonehara S, Odagiri T, Tashiro M, Sata T, Hasegawa H, Seino KI.** 2008. Mechanism of NKT cell activation by intranasal coadministration of alpha-galactosylceramide, which can induce cross-protection against influenza viruses. Mucosal Immunol **1:**208-218.

45. **Guillonneau C, Mintern JD, Hubert FX, Hurt AC, Besra GS, Porcelli S, Barr IG, Doherty PC, Godfrey DI, Turner SJ.** 2009. Combined NKT cell activation and influenza virus vaccination boosts memory CTL generation and protective immunity. Proc Natl Acad Sci U S A **106:**3330-3335.

46. **Albina E, Piriou L, Hutet E, Cariolet R, L'Hospitalier R.** 1998. Immune responses in pigs infected with porcine reproductive and respiratory syndrome virus (PRRSV). Vet Immunol Immunopathol **61:**49-66.

47. **Van Reeth K, Labarque G, Nauwynck H, Pensaert M.** 1999. Differential production of proinflammatory cytokines in the pig lung during different respiratory virus infections: correlations with pathogenicity. Res Vet Sci **67:**47-52.

48. **Buddaert W, Van Reeth K, Pensaert M.** 1998. In vivo and in vitro interferon (IFN) studies with the porcine reproductive and respiratory syndrome virus (PRRSV). Adv Exp Med Biol **440:**461-467.

49. **Miller LC, Laegreid WW, Bono JL, Chitko-McKown CG, Fox JM.** 2004. Interferon type I response in porcine reproductive and respiratory syndrome virus-infected MARC-145 cells. Arch Virol **149:**2453-2463.

50. **Luo R, Xiao S, Jiang Y, Jin H, Wang D, Liu M, Chen H, Fang L.** 2008. Porcine reproductive and respiratory syndrome virus (PRRSV) suppresses interferon-beta production by interfering with the RIG-I signaling pathway. Mol Immunol **45:**2839-2846.

51. **Donelan NR, Basler CF, Garcia-Sastre A.** 2003. A recombinant influenza A virus expressing an RNA-binding-defective NS1 protein induces high levels of beta interferon and is attenuated in mice. J Virol **77:**13257-13266.

52. **Talon J, Salvatore M, O'Neill RE, Nakaya Y, Zheng H, Muster T, Garcia-Sastre A, Palese P.** 2000. Influenza A and B viruses expressing altered NS1 proteins: A vaccine approach. Proc Natl Acad Sci U S A **97:**4309-4314.

53. **Valarcher JF, Furze J, Wyld S, Cook R, Conzelmann KK, Taylor G.** 2003. Role of alpha/beta interferons in the attenuation and immunogenicity of recombinant bovine respiratory syncytial viruses lacking NS proteins. J Virol **77:**8426-8439.

54. **Zust R, Cervantes-Barragan L, Kuri T, Blakqori G, Weber F, Ludewig B, Thiel V.** 2007. Coronavirus non-structural protein 1 is a major pathogenicity factor: implications for the rational design of coronavirus vaccines. PLoS Pathog **3:**e109.

55. **Frias-Staheli N, Giannakopoulos NV, Kikkert M, Taylor SL, Bridgen A, Paragas J, Richt JA, Rowland RR, Schmaljohn CS, Lenschow DJ, Snijder EJ, Garcia-Sastre A, Virgin HWt.** 2007. Ovarian tumor domain-containing viral proteases evade ubiquitin- and ISG15-dependent innate immune responses. Cell Host Microbe **2:**404-416.

56. **Sun Z, Chen Z, Lawson SR, Fang Y.** 2010. The cysteine protease domain of porcine reproductive and respiratory syndrome virus nonstructural protein 2 possesses deubiquitinating and interferon antagonism functions. J Virol **84:**7832-7846.
57. **Sun Z, Li Y, Ransburgh R, Snijder EJ, Fang Y.** 2012. Nonstructural protein 2 of porcine reproductive and respiratory syndrome virus inhibits the antiviral function of interferon-stimulated gene 15. J Virol **86:**3839-3850.
58. **van Kasteren PB, Bailey-Elkin BA, James TW, Ninaber DK, Beugeling C, Khajehpour M, Snijder EJ, Mark BL, Kikkert M.** 2013. Deubiquitinase function of arterivirus papain-like protease 2 suppresses the innate immune response in infected host cells. Proc Natl Acad Sci U S A **110:**E838-847.
59. **Manickam C, Dwivedi V, Patterson R, Papenfuss T, Renukaradhya GJ.** 2013. Porcine reproductive and respiratory syndrome virus induces pronounced immune modulatory responses at mucosal tissues in the parental vaccine strain VR2332 infected pigs. Vet Microbiol **162:**68-77.
60. **Schroder K, Hertzog PJ, Ravasi T, Hume DA.** 2004. Interferon-gamma: an overview of signals, mechanisms and functions. J Leukoc Biol **75:**163-189.
61. **De Bruin TG, Van Rooij EM, De Visser YE, Bianchi AT.** 2000. Cytolytic function for pseudorabies virus-stimulated porcine CD4+ CD8dull+ lymphocytes. Viral Immunol **13:**511-520.
62. **Franzoni G, Kurkure NV, Essler SE, Pedrera M, Everett HE, Bodman-Smith KB, Crooke HR, Graham SP.** 2013. Proteome-wide screening reveals immunodominance in the CD8 T cell response against classical swine fever virus with antigen-specificity dependent on MHC class I haplotype expression. PLoS One **8:**e84246.
63. **Takamatsu HH, Denyer MS, Lacasta A, Stirling CM, Argilaguet JM, Netherton CL, Oura CA, Martins C, Rodriguez F.** 2013. Cellular immunity in ASFV responses. Virus Res **173:**110-121.
64. **Binjawadagi B, Dwivedi V, Manickam C, Ouyang K, Wu Y, Lee LJ, Torrelles JB, Renukaradhya GJ.** 2014. Adjuvanted poly(lactic-co-glycolic) acid nanoparticle-entrapped inactivated porcine reproductive and respiratory syndrome virus vaccine elicits cross-protective immune response in pigs. Int J Nanomedicine **9:**679-694.
65. **Wang S, Fan Y, Brunham RC, Yang X.** 1999. IFN-gamma knockout mice show Th2-associated delayed-type hypersensitivity and the inflammatory cells fail to localize and control chlamydial infection. Eur J Immunol **29:**3782-3792.
66. **Song Z, Wu H, Ciofu O, Kong KF, Hoiby N, Rygaard J, Kharazmi A, Mathee K.** 2003. Pseudomonas aeruginosa alginate is refractory to Th1 immune response and impedes host immune clearance in a mouse model of acute lung infection. J Med Microbiol **52:**731-740.
67. **Diaz MA, Villalobos N, de Aluja A, Rosas G, Gomez-Conde E, Hernandez P, Larralde C, Sciutto E, Fragoso G.** 2003. Th1 and Th2 indices of the immune response in pigs vaccinated against Taenia solium cysticercosis suggest various host immune strategies against the parasite. Vet Immunol Immunopathol **93:**81-90.

940 **FIGURE LEGEND**

941 **Figure 1**. Mutations in GKYLQRRLQ motif impair nsp1β's inhibitory effect on type I interferon
942 production and signaling. HEK-293T cells in 24-well plate were co-transfected with a plasmid
943 expressing WT nsp1β or nsp1β mutant, p125-luc reporter plasmid expressing firefly luciferase
944 under the control of IFN-β promoter (**A**) or pISRE-luc expressing firefly luciferase derived by
945 interferon stimulated response element (ISRE; **B**). Empty vector was used as control. At 24 h
946 post-transfection, cells were stimulated with SeV at 100 HA units/ml or stimulated with IFN-β at
947 2000 IU/ml for 16 h. Cell lysates were harvested for measuring luciferase activity. (**C**) The
948 expression level of nsp1β was evaluated by western blot analysis using nsp1β-specific mAb 123-
949 128, whereas β-tubulin was detected as a loading control. The membrane was incubated with
950 primary antibodies mixture of anti-FLAG M2 mAb (Sigma-Aldrich, St. Louis, MO) and mAb
951 against β-tubulin. Secondary antibody IRDye® 800CW Goat anti-Mouse IgG (H + L) (LI-COR
952 Biosciences, Lincoln, NE) was used for visualizing the target proteins with a digital image
953 system (Odyssey infrared imaging system; LI-COR Biosciences, Lincoln, NE). The expression
954 of nsp1β was quantified and normalized to β-tubulin, and the relative expression levels were
955 showed under each band. Statistical significance between wild type group and mutant virus
956 group was determined by one-way ANOVA and Tukey's test, and indicated with asterisk (*,
957 $p<0.05$; **, $p<0.01$; ***, $p<0.001$).

958 **Figure 2**. Mutations at R128 and R129 in GKYLQRRLQ motif impair the expression of nsp2TF
959 in vaccinia/T7 expression system. HEK-293T cells were infected with vaccinia virus expressing
960 T7 polymerase at 10 MOI, and then transfected with pLnsp1β-2 constructs at 1 h post-infection.
961 The cell lysates were harvested at 18 h post-transfection. (**A**) The nsp2TF was
962 immunoprecipitated by polyclonal antibody (pAb-TF) that specifically recognizes the C-terminal

963 region of nsp2TF using equal amount of lysate. Immunoprecipitated proteins were detected by
964 WB using pAb-TF (top panel) and mAb 140-68 recognizing the common N-terminal region of
965 nsp2-related proteins (bottom panel); (**B**) Western blot detecting the expression of nsp2 (top
966 panel), nsp1β (button panel) using specific mAbs.

967 **Figure 3**. *In vitro* characterization of recombinant viruses containing nsp1β mutations. (**A**)
968 Multiple-step virus growth curve. Each data point shown represents a mean value from
969 duplicates, and error bars show standard errors of the mean (SEM). (**B**) Plaque morphology of
970 WT and recombinant viruses containing mutations in the GKYLQRRLQ motif of nsp1β.

971 **Figure 4**. Mutations in GKYLQRRLQ motif attenuate the ability of PRRSV to suppress the
972 expression of IFN-α and ISGs. Porcine alveolar macrophages seeded in 24-well plate were
973 infected with the WT virus or nsp1β mutants at a MOI of 1.0, and cell culture supernatants were
974 harvested at 12 h post-infection. (**A**) IFN-α production was quantified by using ProcartaPlex
975 Porcine IFN alpha Simplex kit (eBioscience, San Diego, CA). Each data point shown represents
976 a mean value from three independent experiments with duplicate, and error bars show SEM. (**B**)
977 The mRNA expression of ISG15 was evaluated by quantitative real-time PCR and normalized to
978 endogenous β-tubulin mRNA. (**C**) The mRNA expression of IFIT1 was evaluated by quantitative
979 real-time PCR and normalized to endogenous β-tubulin mRNA. (**D**) The mRNA expression of
980 IFITM1 was evaluated by quantitative real-time PCR and normalized to endogenous β-tubulin
981 mRNA. Values (B, C, and D) are expressed as the means ± SEM from three independent
982 experiments. (**E**) The expression of nsp1β at 12 h post-infection was determined by western blot
983 analysis with nsp1β-specific mAb 123-128, whereas β-tubulin was detected as a loading control.
984 The membrane was incubated with primary antibodies mixture of mAb123-128 and mAb against
985 β-tubulin. Secondary antibody IRDye® 800CW Goat anti-Mouse IgG (H + L) (LI-COR

Biosciences, Lincoln, NE) was used for visualizing the target proteins with a digital image system (Odyssey infrared imaging system; LI-COR Biosciences, Lincoln, NE). Statistical significance between wild type group and mutant virus group was determined by one-way ANOVA and Tukey's test, and indicated with asterisk (*, $p<0.05$; **, $p<0.01$; ***, $p<0.001$).

Figure 5. Comparison of viral load in serum samples from pigs inoculated with WT virus and nsp1β mutants. Pigs were uninfected (mock), infected with WT PRRSV (WT), or three indicated mutants (vR128A, vR129A, vRR129AA). Serum samples were collected on the indicated DPIs. (**A**) Viral load in serum samples quantified by quantitative RT-PCR and calculated as viral RNA copies/ml. (**B**) Infectious virus titer in serum samples determined by micro-titration assay and calculated as log$TCID_{50}$/ml. Statistical significance between wild type group and mutant virus group was determined by one-way ANOVA and Tukey's test, and indicated with asterisk (*, $p<0.05$; **, $p<0.01$; ***, $p<0.001$).

Figure 6. Comparison of viral load in BALF and lung samples from pigs inoculated with WT virus and nsp1β mutants. Pigs were uninfected (mock), infected with WT PRRSV (WT), or three indicated mutants (vR128A, vR129A, vRR129AA). The lung harvested on the day of necropsy (7, 21 and 35 DPI) was used in BALF and lung lysate preparation. (**A and B**) Viral load in BALF (**A**) and lung lysate (**B**) samples was quantified by quantitative RT-PCR and calculated as viral RNA copies/ml BALF or viral RNA copies/g lung. (**C and D**) Infectious virus titer in BALF (**C**) and lung lysate (**D**) samples was determined by micro-titration assay and calculated as log$TCID_{50}$/ml or log$TCID_{50}$/g. A legend explaining the treatment groups in panels (**B**), (**C**), and (**D**) is given in panel (**A**). Statistical significance between wild type group and mutant virus group was determined by one-way ANOVA and Tukey's test, and indicated with asterisk (*, $p<0.05$; **, $p<0.01$; ***, $p<0.001$).

1009 **Figure 7**. Comparison of IFN-α production levels and NK cell cytotoxicity in pigs inoculated
1010 with WT virus and nsp1β mutants. Pigs were uninfected (mock), infected with WT PRRSV
1011 (WT), or three indicated mutants (vR128A, vR129A, vRR129AA). **(A)** The lung samples
1012 collected at 7 DPI were used to prepare lung lysates, and IFN-α levels were analyzed by ELISA.
1013 **(B and C)** PBMCs (NK effectors) were harvested on the day of necropsy (7 DPI), and cells were
1014 co-cultured with target cells (K562) at E:T ratio of 100:1(**B**) or 50:1(**C**). After overnight
1015 incubation, the NK specific cytotoxic activity was determined by flow cytometry. Each data
1016 point represents a mean value ± SEM from 3 pigs. Statistical significance between wild type
1017 group and mutant virus group was determined by one-way ANOVA and Tukey's test, and
1018 indicated with asterisk (*, $p<0.05$; **, $p<0.01$; ***, $p<0.001$).

1019 **Figure 8**. Comparison of IFN-γ production levels in pigs inoculated with WT virus and nsp1β
1020 mutants. Pigs were uninfected (mock), infected with WT PRRSV (WT), or three indicated
1021 mutants (vR128A, vR129A, vRR129AA). Blood samples were collected on the indicated DPIs,
1022 and the BALF and lung lysate were prepared using lungs harvested on the day of necropsy (7, 21
1023 and 35 DPI). IFNγ levels in (**A**) Serum and (**B**) Lung lysate, and IL-6 levels in (**C**) BALF and
1024 (**D**) Lung lysate were analyzed by ELISA. Each data point represents a mean value ± SEM from
1025 3 pigs. Statistical significance between wild type group and mutant virus group was determined
1026 by one-way ANOVA and Tukey's test, and indicated with asterisk (*, $p<0.05$; **, $p<0.01$; ***,
1027 $p<0.001$).

1028 **Figure 9.** T-helper and Memory T cells responses in pigs infected with nsp1β mutants. PBMCs
1029 collected at 7, 21 and 35 DPI were unstimulated or restimulated with the respective WT or
1030 mutant viruses that were used to infect pigs. Cells were immunostained for pig specific markers

CD3, CD4, and CD8α, followed by intracellular IFN-γ detection. Frequency of each lymphocyte subset based on the combination of markers are grouped: (**A**) $CD3^{+}CD4^{-}CD8\alpha^{+}$ (CTL/γδ T cells); (**B**) $CD3^{+}CD4^{-}CD8\alpha^{+}IFN\gamma^{+}$ (activated CTL/γδ T cells); **(C)** $CD3^{+}CD4^{+}CD8\alpha^{+}$ (T-helper/Memory cells); (**D**) $CD3^{+}CD4^{+}CD8\alpha^{+}IFN\gamma^{+}$ (activated T-helper/Memory cells) and (**E**) $CD3^{-}CD8\alpha^{+}IFN\gamma^{+}$ (activated NK cells) were analyzed by flow cytometry. A legend explaining the treatment groups in panels (**A**), (**B**), (**D**), and (**E**) is given in panel (**C**). Each bar is the mean value ± SEM of 3 pigs. Statistical significance between wild type and mutant virus-infected pig groups was determined by one-way ANOVA and followed by Tukey's t-test, and indicated with asterisk (*, $p<0.05$; **, $p<0.01$; ***, $p<0.001$).

Table 1. Experimental design for testing of nsp1β mutants in nursery pigs

		Pig Number				
	dpi	Negative control (group 1)	WT[e] (group 2)	R128A (group 3)	R129A (group 4)	RR129AA (group 5)
Blood collection[a]	0	1 ~ 9[c]	10 ~ 18	19 ~ 27	28 ~ 36	37 ~ 45
	1	1 ~ 9	10 ~ 18	19 ~ 27	28 ~ 36	37 ~ 45
	2	1 ~ 9	10 ~ 18	19 ~ 27	28 ~ 36	37 ~ 45
	5	1 ~ 9	10 ~ 18	19 ~ 27	28 ~ 36	37 ~ 45
	14	4 ~ 9	14 ~ 18	22 ~ 27	31 ~ 36	40 ~ 45
	28	7 ~ 9	17, 18	25 ~ 27	34 ~ 36	43 ~ 45
Animal termination[b]	7	1 ~ 3[d]	10, 11, 13	19 ~ 21	28 ~ 30	37 ~ 39
	21	4 ~ 6	14 ~ 16	22 ~ 24	31 ~ 33	40 ~ 42
	35	7 ~ 9	17, 18	25 ~ 27	34 ~ 36	43 ~ 45

a: At 0, 1, 2, 5, 14, and 28 dpi, plasma and PBMCs were collected;

b: At 7, 21, and 35 dpi, 3 pigs from each group were terminated, and their plasma, PBMCs, bronchoalveolar lavage fluid and lung tissue samples were collected;

c: Pigs for blood collection at indicated time point;

d: Pigs terminated at indicated time point;

e: Pig #12 died before 7 dpi

Table 2. Sequence analysis of nsp1β coding region in viruses recovered from infected pigs

Group	Pig #	Designed Mutation	2nd site Mutation
14 days post infection			
vR129A	31	reversion (GCG to AGG)	
	32	stable	122[a]: UCU to CCU[b], Ser to Pro[c]
	33	stable	122: UCU to CCU, Ser to Pro
	34	stable	122: UCU to CCU, Ser to Pro
	35	stable	122: UCU to CCU, Ser to Pro
	36	stable	122: UCU to CCU, Ser to Pro
21 days post infection			
WT	14		9: GAC to GGC, Asp to Gly
	15		9: GAC to GGC, Asp to Gly
	16		9: GAC to GGC, Asp to Gly
vR128A	22	stable	9: GAC to GGC, Asp to Gly; 122: UCU to CCU, Ser to Pro
	23	stable	9: GAC to GGC, Asp to Gly; 122: UCU to CCU, Ser to Pro
	24	stable	9: GAC to GGC, Asp to Gly; 109: CAU to C(A/G)U, His to His/Arg; 122: UCU to CCU, Ser to Pro; 141: CUA to C(U/C)A, Leu to Leu/Pro
vR129A	31	reversion (GCG to AGG)	9: GAC to GGC, Asp to Gly
	32	stable	9: GAC to GGC, Asp to Gly; 87: GAA to GA(A/G); 122: UCU to CCU, Ser to Pro
	33	stable	9: GAC to GGC, Asp to Gly; 122: UCU to CCU, Ser to Pro; 169: UCU to (C/U)CU, Ser to Ser/Pro
vRR129AA	40	stable	
	41	stable	
	42	stable	
35 days post infection			
WT	17		9: GAC to GGC, Asp to Gly; 126: CUA to CU(A/G)
	18		9: GAC to GGC, Asp to Gly
vR128A	27	stable	9: GAC to GGC, Asp to Gly; 109: CAU to CGU, His to Arg; 122: UCU to CCU, Ser to Pro
vR129A	34	stable	9: GAC to GGC, Asp to Gly; 122: UCU to CCU, Ser to Pro; 132: UUU to (G/U)UU, Phe to Val;

vR129A	34		141: CUA to CU(A/G) 169: UCU to (C/U)CU, Ser to Ser/Pro
	35	stable	9: GAC to GGC, Asp to Gly; 122: UCU to CCU, Ser to Pro;
	36	stable	9: GAC to GGC, Asp to Gly; 122: UCU to CCU, Ser to Pro; 169: UCU to CCU, Ser to Pro
vRR129AA	44	stable	9: GAC to GGC, Asp to Gly
	45	stable	9: GAC to GGC, Asp to Gly

a. Numbers refer to codon position in nsp1β coding region; b. Nucleotide substitution; c. Amino acid substitution.

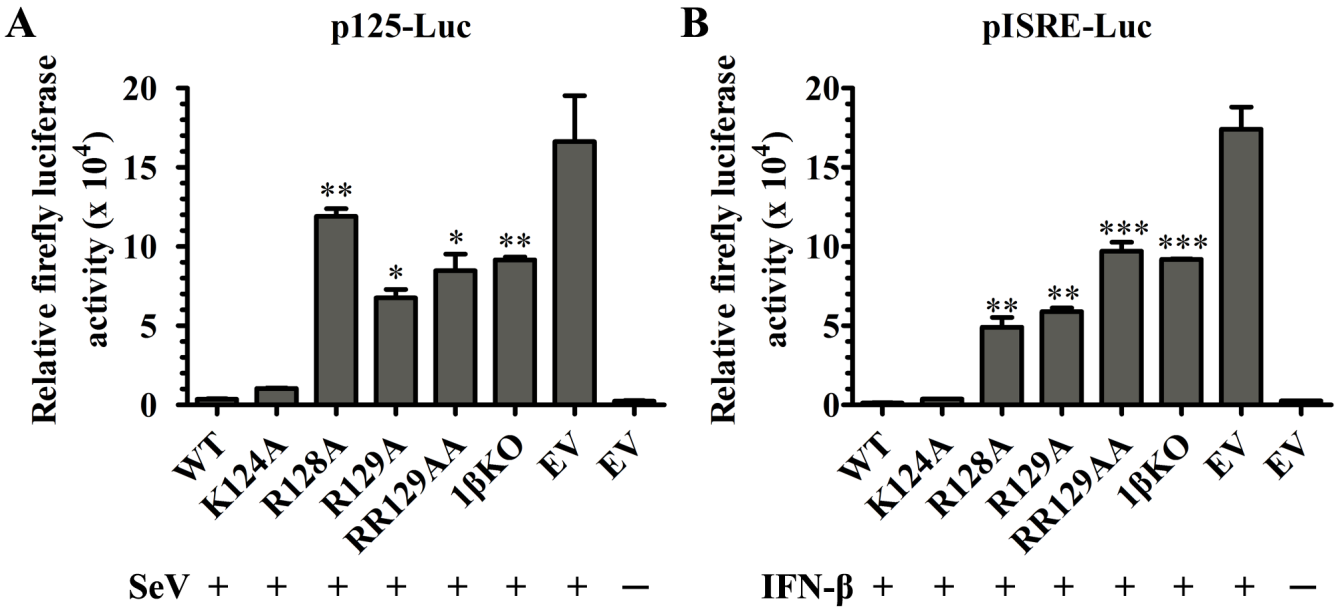

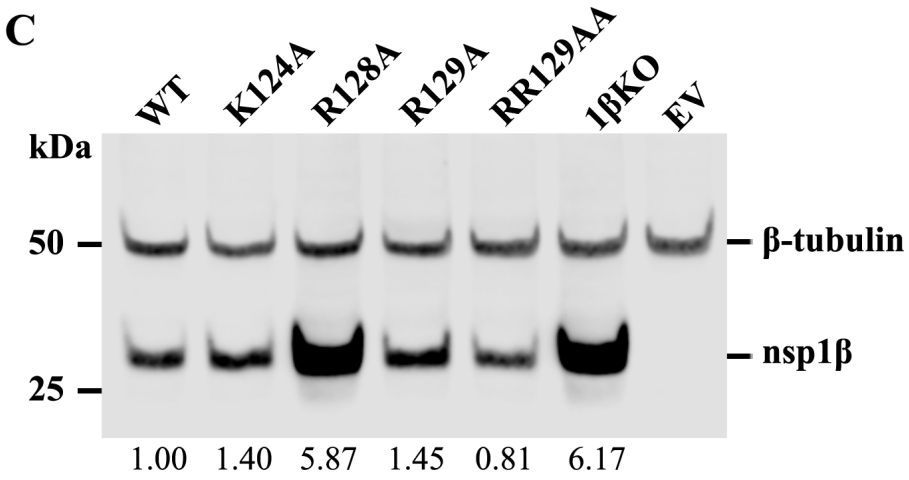

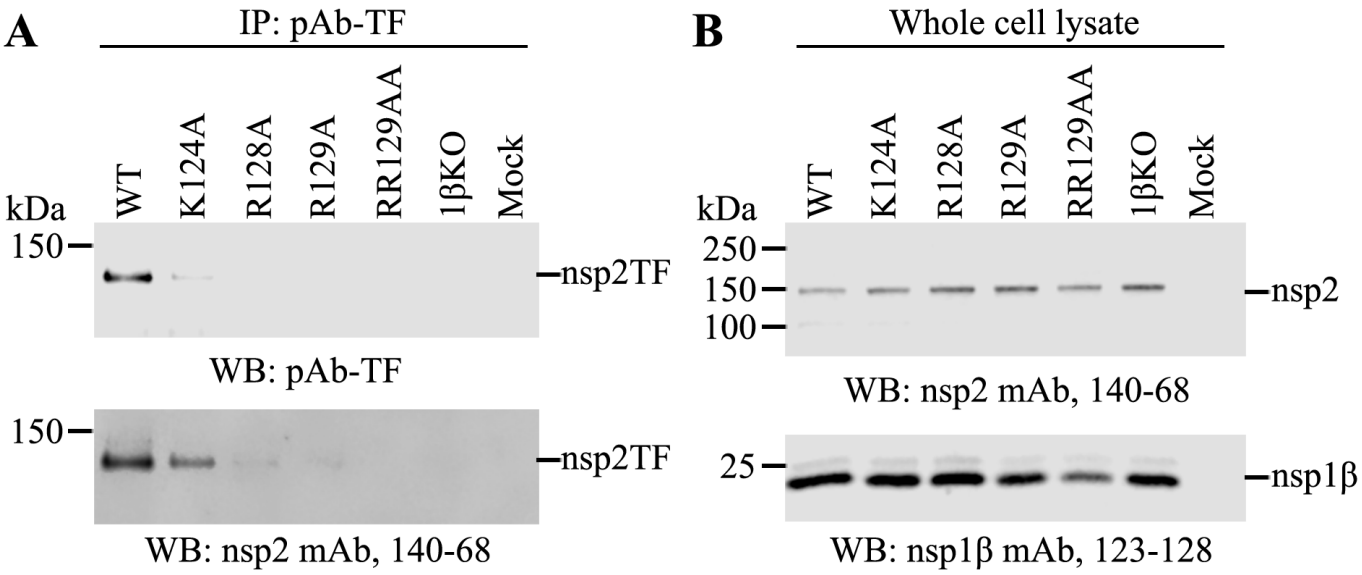

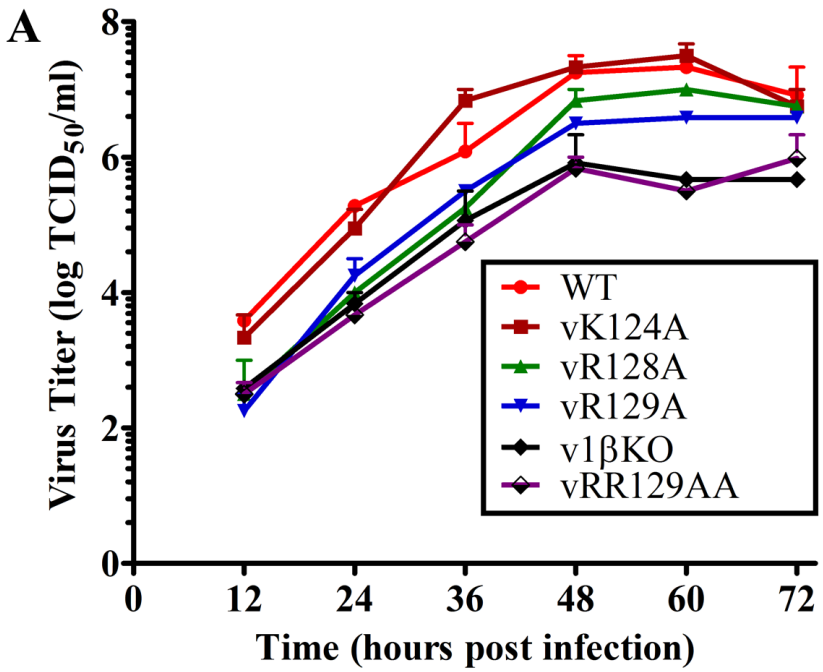

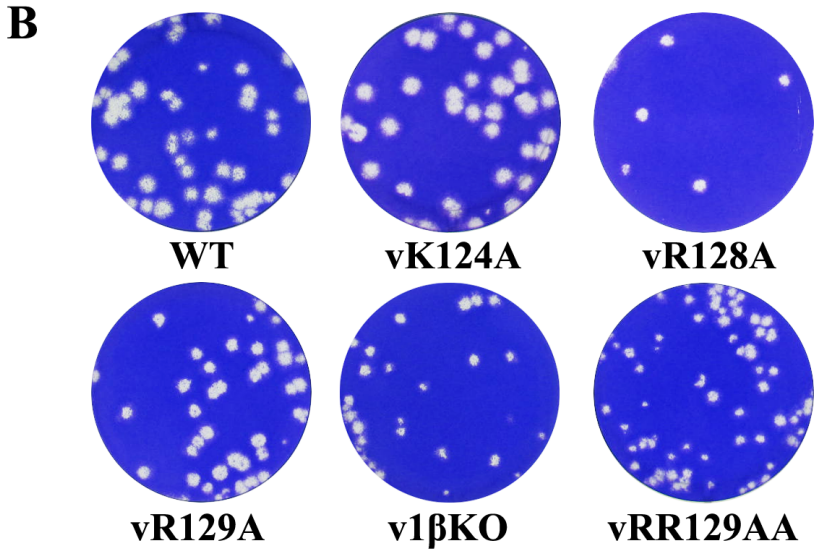

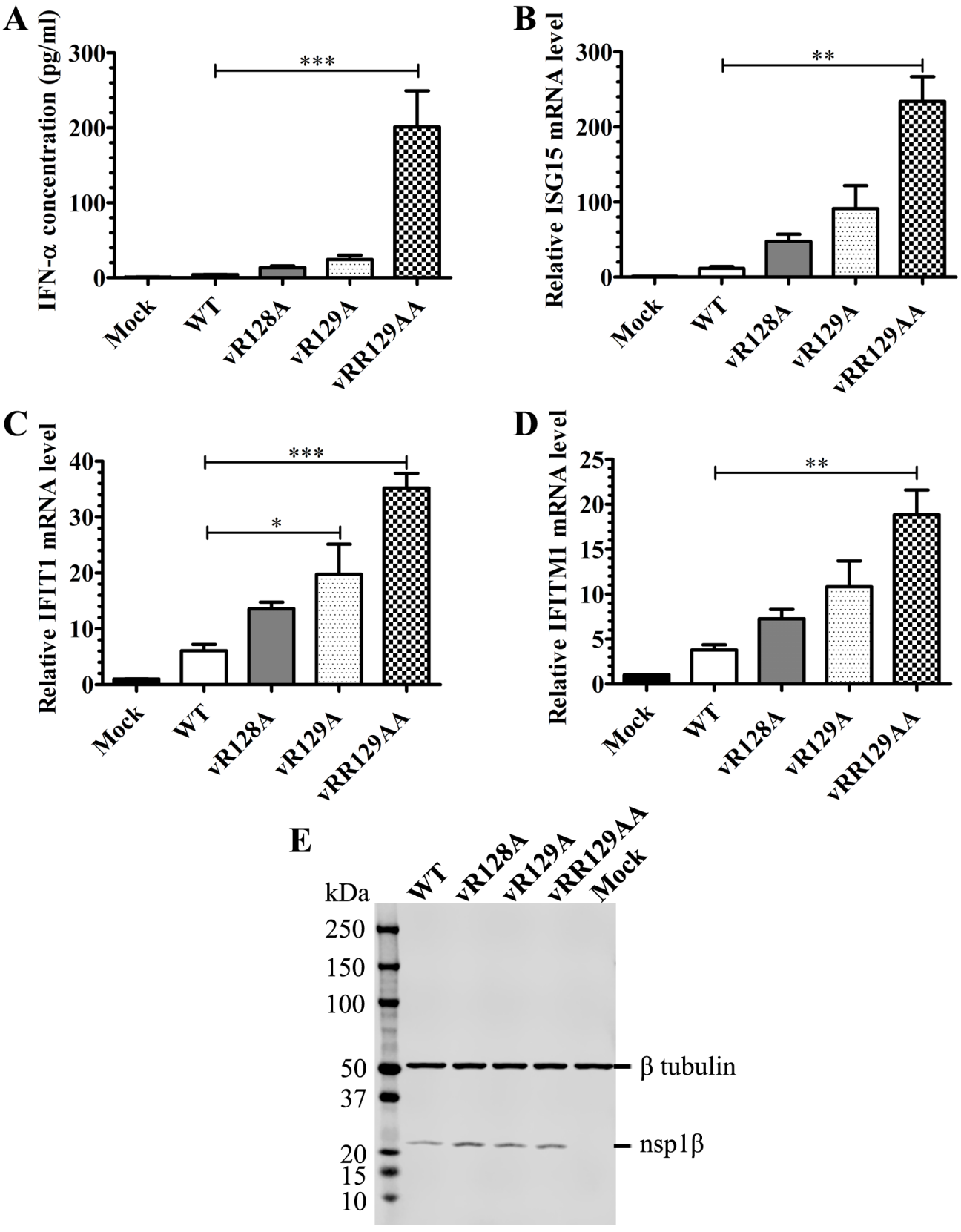

WB: nsp1β mAb, 123-128; α-β tubulin